

Manuscript Number:	GIGA-D-17-00149R2	
Full Title:	Advanced lesion symptom mapping analyses and implementation as BCBtoolkit	
Article Type:	Technical Note	
Funding Information:	Agence Nationale de la Recherche (ANR-09-RPDOC-004-01)	Dr. Emmanuelle Volle
	Agence Nationale de la Recherche (ANR-13- JSV4-0001-01)	Dr. Michel Thiebaut de Schotten
	Agence Nationale de la Recherche (ANR-10-IAIHU-06)	Not applicable
	Fondation pour la Recherche Médicale (FRM DEQ20150331725)	Pr. Richard Levy
Abstract:	<p>Background: Patients with brain lesions provide a unique opportunity to understand the functioning of the human mind. However, even when focal, brain lesions have local and remote effects that impact functionally and structurally connected circuits. Similarly, function emerges from the interaction between brain areas rather than their sole activity. For instance, category fluency requires the association between executive, semantic and language production functions.</p> <p>Findings: Here we provide, for the first time, a set of complementary solutions to measure the impact of a given lesion upon the neuronal circuits. Our methods, which were applied to 37 patients with a focal frontal brain lesion, revealed a large set of directly and indirectly disconnected brain regions that had significantly impacted category fluency performance. The directly disconnected regions corresponded to areas that are classically considered as functionally engaged in verbal fluency and categorization tasks. These regions were also organized into larger directly and indirectly disconnected functional networks, including the left ventral fronto-parietal network, whose cortical thickness correlated with performance on category fluency.</p> <p>Conclusions: The combination of structural and functional connectivity together with cortical thickness estimates reveals the remote effects of brain lesions, provide for the identification of the affected networks and strengthen our understanding of their relationship with cognitive and behavioural measures. The methods presented are available and freely accessible in the BCBtoolkit as supplementary software (http://toolkit.bcblab.com).</p>	
Corresponding Author:	Michel Thiebaut de Schotten CNRS Délégation Paris B Paris, Île-de-France FRANCE	
Corresponding Author Secondary Information:		
Corresponding Author's Institution:	CNRS Délégation Paris B	
Corresponding Author's Secondary Institution:		
First Author:	Chris Foulon	
First Author Secondary Information:		
Order of Authors:	Chris Foulon	
	Leonardo Cerliani	
	Serge Kinkingnéhun	
	Richard Levy	
	Charlotte Rosso	
	Marika Urbanski	

	Emmanuelle Volle
	Michel Thiebaut de Schotten
Order of Authors Secondary Information:	
Response to Reviewers:	<p>Dear dr. Zauner,</p> <p>Thank you for considering our manuscript untitled 'Advanced lesion symptom mapping analyses and implementation as BCBtoolkit' for a technical report in Gigascience. Additionally, we wish to mention again that we will be happy to be included in the thematic series 'Brainhack: Open tools for Brain Science'</p> <p>Concerning your question, I am afraid there is no protected data access scheme. This is because of the wording of the consent. We are sorry we could not find any way around this.</p> <p>Please find below our point by point response to the minor suggestions of reviewer 1.</p> <p>We are looking forward to your assessment.</p> <p>Sincerely,</p> <p>Michel Thiebaut de Schotten</p> <p>1) The He article is cited under lesion-driven tractography but I believe this was a fcMRI study. Actually, He article includes tractography as well as fcMRI. Results are reported in figure 7B of their paper.</p> <p>2) The authors could clarify the comment about how much variance in fcMRI data is explained by the three network model. Thanks for mentioning this was unclear. We modified the text accordingly.</p> <p>3) It's not clear to me why Shannon entropy is included in the 'Structural changes in disconnected regions' section. It is a functional measure and perhaps a separate paragraph is warranted. Apologies if this is confusing. Although Shannon entropy was derived from functional MRI, it is not a functional measure since it was acquired at rest (= no function) in order to estimate the intrinsic connectivity. We strongly believe it should remain in the structural section of the manuscript. This point is defended in the method section of the manuscript as follows: "In the context of rs-fMRI, the entropy measures the local complexity of the Blood Oxygen Level Dependent (BOLD) signal as a surrogate of the complexity of the spontaneous neuronal activity [76, 77]. Since "cells that fire together wire together" [78], for each grey matter voxel Shannon entropy of rs-fMRI can be considered as a surrogate for the complexity of the connections within this voxel and between this voxel and the rest of the brain."</p> <p>4) Page 21, line 1. I think the authors meant to comment on adequate lesion coverage of the entire brain and not lesions that involve the entire brain. Thanks for noticing this mistake! This has now been amended in the manuscript.</p>
Additional Information:	
Question	Response
Are you submitting this manuscript to a special series or article collection?	No
Experimental design and statistics	Yes
Full details of the experimental design and statistical methods used should be given in the Methods section, as detailed in our	

<p>Minimum Standards Reporting Checklist. Information essential to interpreting the data presented should be made available in the figure legends.</p> <p>Have you included all the information requested in your manuscript?</p>	
<p>Resources</p> <p>A description of all resources used, including antibodies, cell lines, animals and software tools, with enough information to allow them to be uniquely identified, should be included in the Methods section. Authors are strongly encouraged to cite Research Resource Identifiers (RRIDs) for antibodies, model organisms and tools, where possible.</p> <p>Have you included the information requested as detailed in our Minimum Standards Reporting Checklist?</p>	<p>Yes</p>
<p>Availability of data and materials</p> <p>All datasets and code on which the conclusions of the paper rely must be either included in your submission or deposited in publicly available repositories (where available and ethically appropriate), referencing such data using a unique identifier in the references and in the “Availability of Data and Materials” section of your manuscript.</p> <p>Have you have met the above requirement as detailed in our Minimum Standards Reporting Checklist?</p>	<p>Yes</p>

Running title: Advanced lesion symptom mapping analyses

1
2 **Advanced lesion symptom mapping analyses and implementation as**
3
4 ***BCBtoolkit***
5
6

7 Foulon C^{a,b,c*}, Cerliani L^{a,b,c}, Kinkingnéhun S^a, Levy R^b, Rosso C^{c,d,e}, Urbanski M^{a,b,f}, Volle
8 E^{a,b,c}, Thiebaut de Schotten M^{a,b,c*}
9

10
11 ^a Brain Connectivity and Behaviour Group, Sorbonne Universities, Paris France.

12 ^b Frontlab, Institut du Cerveau et de la Moelle épinière (ICM), UPMC UMRS 1127, Inserm U
13 1127, CNRS UMR 7225, Paris, France.
14

15 ^c Centre de Neuroimagerie de Recherche CENIR, Groupe Hospitalier Pitié-Salpêtrière, Paris,
16 France.
17

18 ^d Abnormal Movements and Basal Ganglia team, Inserm U 1127, CNRS UMR 7225,
19 Sorbonne Universities, UPMC Univ Paris 06, Institut du Cerveau et de la Moelle épinière,
20 ICM, Paris, France
21

22 ^e APHP, Urgences Cérébro-Vasculaires, Groupe Hospitalier Pitié-Salpêtrière, Paris, France.
23

24 ^f Medicine and Rehabilitation Department, Hôpitaux de Saint-Maurice, Saint-Maurice,
25 France.
26

27
28
29
30
31
32
33
34
35 * Corresponding authors hd.chrisfoulon@gmail.com and michel.thiebaut@gmail.com
36

37
38
39 **Competing interests:**
40

41
42 The authors declare that they have no competing interests
43
44
45
46
47
48
49
50
51
52
53
54
55
56
57
58
59
60
61
62
63
64
65

1
2 **Abstract**
3

4 **Background:** Patients with brain lesions provide a unique opportunity to understand the
5 functioning of the human mind. However, even when focal, brain lesions have local and
6 remote effects that impact functionally and structurally connected circuits. Similarly, function
7 emerges from the interaction between brain areas rather than their sole activity. For instance,
8 category fluency requires the association between executive, semantic and language
9 production functions.
10

11 **Findings:** Here we provide, for the first time, a set of complementary solutions to measure
12 the impact of a given lesion upon the neuronal circuits. Our methods, which were applied to
13 37 patients with a focal frontal brain lesion, revealed a large set of directly and indirectly
14 disconnected brain regions that had significantly impacted category fluency performance.
15 The directly disconnected regions corresponded to areas that are classically considered as
16 functionally engaged in verbal fluency and categorization tasks. These regions were also
17 organized into larger directly and indirectly disconnected functional networks, including the
18 left ventral fronto-parietal network, whose cortical thickness correlated with performance on
19 category fluency.
20

21 **Conclusions:** The combination of structural and functional connectivity together with
22 cortical thickness estimates reveals the remote effects of brain lesions, provide for the
23 identification of the affected networks and strengthen our understanding of their relationship
24 with cognitive and behavioural measures. The methods presented are available and freely
25 accessible in the *BCBtoolkit* as supplementary software [1].
26
27
28
29
30

31
32 **Keywords**
33

34 Brain, MRI, Lesion, Statistics, Software, Open source, Connectivity, Disconnection,
35 Behaviour
36
37
38
39
40
41
42
43
44
45
46
47
48
49
50
51
52
53
54
55
56
57
58
59
60
61
62
63
64
65

1
2
3
4
5
6
7
8
9
10
11
12
13
14
15
16
17
18
19
20
21
22
23
24
25
26
27
28
29
30
31
32
33
34
35
36
37
38
39
40
41
42
43
44
45
46
47
48
49
50
51
52
53
54
55
56
57
58
59
60
61
62
63
64
65

Recent advances in neuroimaging techniques, allowed for the further examination of the structural and the functional organization of the human brain. While diffusion weighted imaging (DWI) tractography [2] depicts how brain areas are connected together, functional magnetic resonance imaging (*fMRI*) measures the activity within and interaction between brain areas in the elaboration of functions [3]. These methods have been successfully applied to the healthy human brain, however, they remain underused in patients with brain lesions.

Patients with brain lesions provide a unique opportunity to understand the functioning of the human mind. Lesion symptom mapping analyses traditionally assume that visible and directly damaged areas are responsible for a patient's symptoms [4-7]. Following this logic, the areas that are the most frequently damaged by the lesion are considered as the neuronal substrate for the function. Previous studies employing this method have pinpointed critical areas dedicated to, for example, language production [8], comprehension [9], spatial awareness [10-13] and other high-level cognitive functions [14-17]. However, anatomical disconnections between regions are also important considerations for the exploration of cognitive deficit [18, 19]. The dysfunction of distant areas that are connected to the lesioned tissue has also been reported in *fMRI* studies. They have shown that the networks are disrupted even by distant lesions through disconnection and diaschisis mechanisms [20-22].

Non-local effects of lesions have previously been explored using various forms of atlas-based analyses of tract damage [23-32], lesion-driven tractography [32-34], disconnectome-mapping [35-39] and lesion-driven resting state *fMRI* (rs-*fMRI*) connectivity [34, 40]. However, determining what these methods actually measure and identifying how to properly combine them are not always fully clear to the scientific community. Furthermore, there is an extremely limited availability of free, open-source software that applies methods to measure the non-local effects of lesions. These resources and scientific tools remain very much inaccessible and present a potential threat to reproducible science [41].

Disconnections and diaschisis can have an impact upon distant regions in several respects through maladaptive responses and pathological spread [42]. When disconnected from its inputs and outputs, a region can no longer contribute to the elaboration of the supported function. This phenomenon is called diaschisis [20, 21, 43]. Once deprived from its inputs

1 and/or outputs, transneuronal degeneration in the region will occur [42], dendrites and
2 synapses density will decrease in number, myelin content will be altered and neurons will
3 reduce in size or die through a mechanism called apoptosis, a programmed cell death [44-46].
4 Hence, a white matter disconnection leads to both functional and anatomical changes that
5 extend well beyond the visible damage. New approaches are therefore required to capture the
6 long-range effects that follow brain disconnections. For instance, cortical thickness [e.g. 47]
7 and other volumetric [e.g. voxel based morphometry 48] analyses have been previously used
8 to study the structural changes associated with brain lesions, but have not been applied in the
9 context of brain disconnection.
10
11
12
13
14
15
16
17

18 In response to this need, we provide here a set of complementary solutions to measure both
19 the circuit, and the subsequent changes within the circuit that is caused by a lesion. We
20 applied these methods to 37 patients with a focal brain lesion following a stroke or a surgical
21 resection. We first assessed the risk of disconnection in well-known white matter tracts and
22 tested their relationship with category fluency performance. Category fluency is an
23 appropriate test to explore disconnection since it requires the association between executive,
24 semantic and language production functions [49, 50]. We then developed a tractography-
25 based approach in order to produce maps of the areas that are directly disconnected by the
26 lesion and tested their relationship with category fluency performance. We additionally
27 calculated the rs-fMRI connectivity of these areas to reveal the whole network of directly and
28 indirectly connected regions that participate in category fluency. Finally, we explored
29 potential microstructural changes in the latter disconnected regions, by estimating neuronal
30 loss or local connectivity degeneration derived from MR-based measures of cortical thickness
31 and resting state fMRI entropy.
32
33
34
35
36
37
38
39
40
41
42
43
44

45 **Methods**

46 *Participants and Category fluency task*

47
48
49 Thirty-seven right-handed patients (French-native speakers; 19 females; mean age 48 ± 14.2
50 years, age ranging from 23 to 75 years) who presented with a frontal lobe lesion at the
51 chronic stage (> 3 months) were included in this study (see table 1 for demographics). These
52 patients were recruited from the stroke unit and the neuroradiology department at Salpêtrière
53
54
55
56
57
58
59
60
61
62
63
64
65

1
2
3
4
5
6
7
8
9
10
11
12
13
14
15
16
17
18
19
20
21
22
23
24
25
26
27
28
29
30
31
32
33
34
35
36
37
38
39
40
41
42
43
44
45
46
47
48
49
50
51
52
53
54
55
56
57
58
59
60
61
62
63
64
65

Hospital, the neurological unit at Saint-Antoine Hospital and the neuroradiology department at Lariboisière Hospital in Paris. Patients with a history of psychiatric or neurological disease, drug abuse, or MRI contraindications were not included. Additionally, we gathered behavioural data from 54 healthy participants (French-native speakers; 27 females; mean age 45.8 ± 14.4 years, age ranging from 22 to 71 years) in order to constitute a normative group.

All participants performed a category fluency task [51] in French. They were instructed to enumerate as many animals as possible during a timed period of 120 seconds. The results were recorded by a clinical neuropsychologist (M.U.). Repetition and declination of the same animal were not taken into account in the final category fluency score.

The experiment was approved by the local ethics committee (Comités de protection des personnes, CPP Ile de France VI, Groupe hospitalier Pitie Salpetriere, Reference project number 16-10); all participants provided written informed consent in accordance to the Declaration of Helsinki. Participants also received a small indemnity for their participation.

Magnetic resonance imaging

An axial three-dimensional magnetization prepared rapid gradient echo (MPRAGE) dataset covering the whole head was acquired for each participant (176 slices, voxel resolution = $1 \times 1 \times 1$ mm, echo time = 3 msec, repetition time = 2300 msec, flip angle = 9°).

Additionally, the same participants underwent an *f*MRI session of resting state. During the resting state session, participants were instructed to relax, keep their eyes closed but to avoid falling asleep. Functional images were obtained using T2-weighted echo-planar imaging (EPI) with blood oxygenation level-dependent contrast using SENSE imaging an echo time of 26 msec and a repetition time of 3000 msec. Each dataset comprised 32 axial slices acquired continuously in ascending order covering the entire cerebrum with a voxel resolution of $2 \times 2 \times 3$ mm. 200 volumes were acquired using these parameters for a total acquisition time of 10 minutes.

Finally, diffusion weighted imaging was also acquired for 54 participants of the normative group (French-native speakers; 27 females; mean age 45.8 ± 14.4 years, age ranging from 22 to 71 years) and consisted in a total of 70 near-axial slices acquired using a fully optimised acquisition sequence for the tractography of diffusion-weighted imaging (DWI), which provided isotropic ($2 \times 2 \times 2$ mm) resolution and coverage of the whole head with a

1
2
3
4
5
6
7
8
9
10
11
12
13
14
15
16
17
18
19
20
21
22
23
24
25
26
27
28
29
30
31
32
33
34
35
36
37
38
39
40
41
42
43
44
45
46
47
48
49
50
51
52
53
54
55
56
57
58
59
60
61
62
63
64
65

posterior-anterior phase of acquisition. The acquisition was peripherally-gated to the cardiac cycle [52] with an echo time = 85 msec. We used a repetition time equivalent to 24 RR (i.e. interval of time between two heart beat waves). At each slice location, 6 images were acquired with no diffusion gradient applied. Additionally, 60 diffusion-weighted images were acquired, in which gradient directions were uniformly distributed on the hemisphere with electrostatic repulsion. The diffusion weighting was equal to a b-value of 1500 sec mm⁻².

Stereotaxic space registration

As spatial normalisation can be affected by the presence of a brain lesion, additional processing was required before calculating the normalisation. For instance, in the case of bilateral lesions, the registration was weighted as previously reported [53]. For unilateral lesions, the first step was to produce an enantiomorphic filling of the damaged area [54]. Each patient's lesion (or signal abnormalities due to the lesion) was manually segmented (using FSLview; <http://fsl.fmrib.ox.ac.uk>). Unilateral lesions were replaced symmetrically by the healthy tissue of the contralateral hemisphere. Enantiomorphic T1 images were fed into FAST [55] for estimation of the bias field and subsequent correction of radiofrequency field inhomogeneity. This improved the quality of the automated skull stripping performed using bet [56] and the registration to the MNI152 using affine and diffeomorphic deformations [57]. The original T1 images (non enantiomorphic) were registered to the MNI152 space using the same affine and diffeomorphic deformations as calculated above. Subsequently, lesions were segmented again in the MNI152 space under the supervision of an expert neurologist (E.V.). This method has been made freely available as the tool *normalisation* as part of *BCBtoolkit* [1].

The following sections of the manuscript are hypotheses-driven and outlined in supplementary figure 1.

White matter tracts disconnection

Each patient's lesion was compared with an atlas of white matter tracts [58], indicating for each voxel, the probability of finding a white matter tract such as the arcuate fasciculus, the frontal aslant tract or the uncinate fasciculus in the MNI152 coordinate system. We considered a tract to be involved when the likelihood of a tract being present in a given voxel

1 was estimated above 50% [23]. This method is freely available as *tractotron* in *BCBtoolkit*
2 [1]. We focused on frontal lobe tracts with a potential effect on executive, semantic and
3 language functions since all of the patients had a frontal lesion. These tracts included the
4 cingulum, the frontal aslant and the frontal superior and inferior longitudinal tracts for the
5 executive functions [59], the uncinate and the inferior fronto-occipital fasciculi for the
6 semantic access [60, 61] and the anterior and long segment of the arcuate fasciculi for the
7 phonemic system [62, 63]. A Kruskal-Wallis test was employed to compare performance on
8 the category fluency test for each tract between both preserved and disconnected patients and
9 control participants. Subsequently, for each significant tract between patients, Mann-Whitney
10 post-hoc comparisons were performed (**Fig.1**).
11
12
13
14
15
16
17
18
19

20 *Direct disconnection of brain areas: structural connectivity network*

21 This approach employed the diffusion weighted imaging datasets of 10 participants in the
22 normative group to track fibres passing through each lesion.
23
24

25 For each participant, tractography was estimated as indicated in [64].

26 Patients' lesions in the MNI152 space were registered to each control native space using
27 affine and diffeomorphic deformations [57], and subsequently, used as seed for the
28 tractography in Trackvis [65]. Tractography from the lesions were transformed in visitation
29 maps [66, 67], binarized and brought to the MNI152 using the inverse of precedent
30 deformations. Finally, we produced a percentage overlap map by summing at each point in
31 the MNI space the normalized visitation map of each healthy subject. Hence, in the resulting
32 *disconnectome map*, the value in each voxel took into account the inter-individual variability
33 of tract reconstructions in controls, and indicated a probability of disconnection from 50 to
34 100% for a given lesion (i.e. thus explaining more than 50% of the variance in disconnection
35 and corresponding to a large effect size). This procedure was repeated for all lesions,
36 allowing the construction of a *disconnectome map* for each patient/lesion. These steps were
37 automatized in the tool *disconnectome map* as part of the *BCBtoolkit*. Note that sample size
38 and age effects were carefully explored and reported in the supplementary material. Overall,
39 10 subjects are sufficient to produce a good enough *disconnectome map* that matches the
40 overall population (more than 70% of shared variance). We also demonstrate in the
41 supplementary material that *disconnectome maps* show a very high anatomical similarity
42 between decades and no decrease of this similarity with age.
43
44
45
46
47
48
49
50
51
52
53
54
55
56
57
58
59
60
61
62
63
64
65

1
2 Thereafter, we used *AnaCOM2* available within the *BCBtoolkit* in order to identify the
3 disconnections that are associated with a given deficit, i.e. connections that are critical for a
4 given function. *AnaCOM2* is comparable to *AnaCOM* [68] but has been reprogrammed and
5 optimised to work on any Linux or Macintosh operating systems.
6
7

8
9 Initially, *AnaCOM* is a cluster-based lesion symptom mapping approach, which identifies
10 clusters of brain lesions that are associated with a given deficit, i.e. the regions that are
11 critical for a given function. In the context of this paper, *AnaCOM2* used *disconnectome*
12 *maps* instead of lesion masks, to identify clusters of disconnection that are associated with
13 category fluency deficits, i.e. the connections that are critical for a given function. Compared
14 to standard VLSM [8], *AnaCOM2* regroups voxels with the same distribution of
15 neuropsychological scores into clusters of voxels. Then, for each cluster above 8mm³,
16 *AnaCOM2* will perform a Kruskal-Wallis test between patients with a disconnection, patients
17 spared of disconnection and controls. Resulting p-values are Bonferroni-Holm corrected for
18 multiple comparisons. Subsequently, significant clusters (p-value < 0.05) are used to perform
19 a post-hoc Mann-Whitney comparison between two subgroups of interest (i.e. disconnected
20 patients and healthy subjects). Post-hoc results are Bonferroni-Holm corrected for multiple
21 comparisons (statistical tests and corrections are computed using R language: [69]).
22
23

24
25 Patients-controls comparisons have been chosen as a first step in order to avoid drastic
26 reduction of statistical power when two or more non-overlapping areas are responsible for
27 patients reduced performance [68]. Non-parametric statistics have been chosen, as it is fair to
28 consider that some clusters will not show a Gaussian distribution. *AnaCOM2* resulted in a
29 statistical map that reveals, for each cluster, the significance of a deficit in patients
30 undertaking a given task as compared to controls.
31
32

33
34 In the following sections of the manuscript, the term clusters systematically refers to the
35 result of the post-hoc Mann-Whitney comparison between disconnected patients and healthy
36 subjects that survived Bonferroni-Holm correction for multiple comparisons.
37
38
39
40
41
42
43

44 *fMRI Meta-analyses*

45
46 A method described by Yarkoni et al. [70, 71] was used to identify the functional networks
47 involved in category fluency. We searched for brain regions that are consistently activated in
48 studies that load highly on 2 features: “fluency” (120 studies, 4214 activations) and
49
50
51
52
53
54
55
56
57
58
59
60
61
62
63
64
65

“category” (287 studies, 10179 activations). The results were superimposed on the 3D reconstruction of the MNI152 images (**Fig. 3**).

Indirect disconnection of brain areas: functional connectivity network

Rs-fMRI images were first motion corrected using MCFLIRT [72], then corrected for slice timing, smoothed with a full half width maximum equal to 1.5 times the largest voxel dimension and finally filtered for low temporal frequencies using a gaussian-weighted local fit to a straight line. These steps are available in Feat as part of FSL package [73].

Rs-fMRI images were linearly registered to the enantiomorphic T1 images, and subsequently to the MNI152 template (2mm) using affine transformations. Confounding signals were discarded from rs-fMRI by regressing out a confound matrix from the functional data. The confound matrix included the estimated motion parameters obtained from the previously performed motion correction, the first eigenvariate of the white matter and cerebrospinal fluid (CSF) as well as their first derivative. Eigenvariables can easily be extracted using `fslmeants` combined with the `--eig` option. White matter and CSF eigenvariables were extracted using masks based on the T1 derived 3-classes segmentation thresholded to a probability value of 0.9, registered to the rs-fMRI images and binarized. Finally, the first derivative of the motion parameters, white matter and CSF signal was calculated by linear convolution between their time course and a $[-1 \ 0 \ 1]$ vector.

For each control participant, we extracted the time course that corresponded to each significant cluster which was identified by the statistical analyses of the *disconnectome maps*. These time courses were subsequently correlated to the rest of the brain so as to extract seed-based resting-state networks. In order to obtain the most representative networks at the group level, for each seed-based resting-state network, we calculated the median network across the group. The median network resulting from a seed contains, in each voxel, the median of functional connectivity across all the control subjects. Medians were chosen instead of average as they are less sensitive to outliers and are more representative of the group level data [74]. The calculation of the functional connectivity was automatized and made available inside the *funcon* tool as part of *BCBtoolkit*. Medians were calculated using the function `fslmaths`.

Visual inspection revealed that several of these resting state networks shared a very similar

1 distribution of activations. Therefore, an ‘activation’ matrix was derived from the seed-based
2 resting-state networks. This matrix consisted of columns that indicated each seed-based
3 resting-state network, and rows that represented the level of activation for each voxel in the
4 cortex. This ‘activation’ matrix was entered into a principal component analysis in SPSS
5 (SPSS, Chicago, IL) using a covariance matrix and varimax rotation (with a maximum of 50
6 iterations for convergence), in order to estimate the number of principal components to
7 extract for each function. Components were plotted according to their eigenvalue (y) (Lower
8 left panel in **Fig. 4**) and we applied a scree test to separate the principal from residual
9 components. This analysis revealed that three factors were enough to explain 82% of the
10 variance of the calculated seed-based resting-state networks. This means that three factors are
11 good enough to summarise most of the seed-based resting-state networks results. Finally,
12 brain regions having a statistically significant relationship with the three components (i.e.
13 factor-networks) were detected using a linear regression with 5.000 permutations, in which
14 the eigenvalues of the three components represented the independent variable and the seed-
15 based resting-state networks the dependent variable. Results were Family Wise Error (FWE)
16 corrected for multiple comparisons, and projected onto the average 3D rendering of the
17 MNI152 template in the top panel of **Fig. 4**. In the following sections of the manuscript, the
18 term factor-networks systematically refers to brain regions having a statistically significant
19 relationship with the three components.
20
21
22
23
24
25
26
27
28
29
30
31
32
33
34
35

36 Additionally, for each patient, we extracted the time course that corresponded to each factor-
37 network. These time courses were subsequently correlated to the rest of the brain so as to
38 extract seed-based factor-networks in each patient. FSLstats was employed to extract the
39 strength of factor-networks functional connectivity and subsequently, to compare patients
40 according to their disconnection status. Note that a patient disconnected in a factor-network is
41 a patient who has a disconnection in at least one of the cluster that contributed significantly to
42 the factor-network.
43
44
45
46
47
48
49
50

51 *Structural changes in disconnected regions*

52 A distant lesion can affect cortical macro and microstructure remotely. Conscious of this, we
53 attempted to estimate these structural changes and their relationship with category fluency
54 within each functional factor-network. To this aim, we explored the properties of each
55
56
57
58
59
60
61
62
63
64
65

1 functional network using two complementary measures: T1w-based cortical thickness to
2 identify fine local volumetric changes and the Shannon entropy of rs-fMRI as a surrogate for
3 the local complexity of the neural networks [75]. Each original functional network seeded
4 from each cluster was thresholded and binarized at $r > 0.3$ and used as a mask to extract
5 cortical thickness and entropy. Patients' lesions were masked out for these analyses.
6
7

8
9 For the cortical thickness, a registration-based method (Diffeomorphic Registration based
10 Cortical Thickness, DiReCT) was employed [76] from the T1-weighted imaging dataset. The
11 first step as for the *normalisation* was to produce an enantiomorphic filling of the damaged
12 area in order to avoid the analysis to be contaminated by the lesioned tissue. The second step
13 of this method consisted in creating two two-voxel thick sheets, one laying just between the
14 grey matter and the white matter and the second laying between the grey matter and the CSF.
15 Then, the grey/white interface was expanded to the grey/CSF interface using diffeomorphic
16 deformation estimated with ANTs. The registration produced a correspondence field that
17 allows an estimate of the distance between the grey/white and the grey/CSF interfaces, and
18 thus corresponded to an estimation of cortical thickness. Voxels belonging to the lesion were
19 subsequently removed from the cortical thickness maps (see **supplementary figure 2**). This
20 approach has good scan-rescan repeatability and good neurobiological validity as it can
21 predict with a high statistical power the age and gender of the participants [77] as well as
22 atrophy following brain lesions [78]. Note that the striatum and the thalamus were excluded
23 from the cortical thickness analysis since they do not have a cortical ribbon.
24
25

26
27 Shannon entropy is an information theory derived measure that estimates signal complexity
28 [79, 80]. In the context of rs-fMRI, the entropy measures the local complexity of the Blood
29 Oxygen Level Dependent (BOLD) signal as a surrogate of the complexity of the spontaneous
30 neuronal activity [81, 82]. Since “cells that fire together wire together” [83], for each grey
31 matter voxel Shannon entropy of rs-fMRI can be considered as a surrogate for the complexity
32 of the connections within this voxel and between this voxel and the rest of the brain. Shannon
33 entropy was extracted from the previously preprocessed rs-fMRI using the following formula:
34 $-\sum(p \cdot \log(p))$ where p indicates the probability of the intensity in the voxel [75].
35
36

37
38 FSLstats was employed to extract the average cortical thickness and resting state fMRI
39 entropy for each cluster and factor-network. Statistical analysis was performed using SPSS
40 software (SPSS, Chicago, IL). In our analysis, Gaussian distribution of the data was not
41 confirmed for the cortical thickness and the entropy measures using the Shapiro–Wilk test.
42
43
44
45
46
47
48
49
50
51
52
53
54
55
56
57
58

1
2 Therefore, non-parametric statistics were chosen to compare cortical thickness and entropy
3 levels between patients disconnected, spared and controls in each cluster and factor network.
4 Additionally, bivariate Spearman rank correlation coefficient analyses were performed
5 between the cortical thickness or entropy measurement of each functional network and each
6 patient's category fluency performance. Correlation significant at $p < 0.0041$ survives
7 Bonferroni correction for multiple comparisons (12 networks).
8
9

10 11 12 **Results**

13 14 15 *White matter tracts disconnection*

16
17 Patients' lesions were compared to an atlas of white matter connections in order to identify
18 the probability of tract disconnections [58]. A Kruskal-Wallis test indicated that for each
19 tract, patients (i.e. connected and disconnected) and control participants showed a
20 significantly different performance on the category fluency test (all $p < 0.001$, full statistics
21 reported in **Table 2**). Between patients, post-hoc comparisons revealed that disconnections of
22 the left frontal aslant ($U = 90.0$; $p = 0.0389$), frontal inferior longitudinal ($U = 69.0$; $p = 0.$
23 0216) and frontal superior longitudinal ($U = 75.0$; $p = 0.0352$) tracts, the anterior ($U = 28.5$;
24 $p = 0.0116$) and long segment ($U = 31.5$; $p = 0.0059$) of the arcuate fasciculus were
25 associated with a poorer performance in category fluency (**Fig. 1**). However, these post-hoc
26 comparisons did not survive Bonferroni-Holm correction for multiple comparisons.
27
28
29
30
31
32
33
34
35
36
37

38
39 These results indicate that poor performance measured in patients with brain damage can be
40 associated to some extent with white matter tract disconnections.
41
42
43
44
45

46 47 *Direct disconnection of brain areas: structural connectivity network*

48
49 As different white matter atlases exist for the interpretation of the white matter tract
50 disconnection [84], and atlas-based approaches cannot assess the disconnection of the
51 subportion of tracts nor the involvement of multiple tracts by a lesion, data driven maps of
52 disconnection or 'disconnectomes' were produced. Using tractography in a group of 10
53 healthy controls, the registered lesions were used as a seed to reveal white matter tracts that
54 passed through the injured area so as to produce maps of disconnections, later referred to as
55
56
57
58
59

1
2
3
4
5
6
7
8
9
10
11
12
13
14
15
16
17
18
19
20
21
22
23
24
25
26
27
28
29
30
31
32
33
34
35
36
37
38
39
40
41
42
43
44
45
46
47
48
49
50
51
52
53
54
55
56
57
58
59
60
61
62
63
64
65

disconnectome maps. Category fluency scores were attributed to each patient's *disconnectome map* (see Fig. 2a). A Kruskal-Wallis test indicated that, for several clusters, patients (i.e. connected and disconnected) and control participants showed a significantly different performance on the category fluency test (all $p < 0.001$, full statistics reported in **Table 3**).

Results were further statistically assessed using Mann-Whitney post-hoc comparisons in order to identify areas that, when deafferented due to a disconnection mechanism, lead to a significant decrease in performance in category fluency when compared to controls.

The following results are Bonferroni-Holm corrected for multiple comparisons. Main cortical areas in the left hemisphere included the pre-supplementary motor area (PreSMA; Cluster size = 1449; Mann Whitney $U = 88.5$; $p = 0.025$), the anterior portion of the intraparietal sulcus (Cluster size = 1143; $U = 18$; $p = 0.030$), anterior (Cluster size = 837; $U = 304$; $p = 0.025$) and the middle (Cluster size = 898; $U = 95.5$; $p = 0.014$) cingulate gyrus, the middle frontal gyrus (MFg, Cluster size = 829; $U = 81.5$; $p = 0.005$), the pars opercularis of the inferior frontal gyrus (Cluster size = 5314; $U = 16$; $p = 0.025$).

In the right hemisphere, the preSMA (Cluster size = 1050; $U = 50.5$; $p = 0.014$), the MFg (Cluster size = 552; $U = 54$; $p = 0.018$), the anterior (Cluster size = 572; $U = 44.5$; $p = 0.009$) and the middle (Cluster size = 817; $U = 317$; $p = 0.041$) cingulate gyrus were also involved (**Fig. 2b**)

Subcortical areas in the left hemisphere involved the caudate, the putamen and several ventral thalamic nuclei including the ventral anterior (VA), the ventrolateral anterior (VLa) and the ventrolateral posterior (VLp) as a part of the same cluster (Cluster size = 5314; $U = 16$; $p = 0.025$)

In the right hemisphere, the striatum (Cluster size = 527; $U = 310$; $p = 0.031$), and the ventral thalamic nuclei (Cluster size = 935; $U = 202.0$; $p = 0.025$) were also involved (**Fig. 2b**).

Additionally, between patients (i.e. connected and disconnected, uncorrected for multiple comparisons) comparisons confirmed the critical involvement of the preSMA ($U = 212$, $p =$

1
2
3
4
5
6
7
8
9
10
11
12
13
14
15
16
17
18
19
20
21
22
23
24
25
26
27
28
29
30
31
32
33
34
35
36
37
38
39
40
41
42
43
44
45
46
47
48
49
50
51
52
53
54
55
56
57
58
59
60
61
62
63
64
65

0.0456) the MFg (U = 237, p = 0.01), the pars opercularis (U = 179, p = 0.004) and the intra-parietal sulcus (IPs, U = 172, p = 0.01) in the left hemisphere. The preSMA (U = 208; p = 0.01) and the MFg (U = 196; p = 0.038) were also involved in the right hemisphere (**Fig. 2c**).

Full statistics are reported in **Table 3**

fMRI Meta-analyses

We further examined whether the disconnected areas in patients with poor performance are functionally engaged in tasks related to fluency and categorization using a meta-analysis approach [70, 71].

The result indicates that disconnected areas reported as significantly contributing to category fluency performance in patients are classically activated by functional MRI tasks requiring either fluency or categorization in healthy controls (**Fig. 3**).

Indirect disconnection of brain areas

As the *disconnectome mapping* method cannot measure the indirect disconnection produced by a lesion (i.e. it fails to measure the disconnection in a region that is not directly, anatomically connected to a damaged area, but that nonetheless remains a part of the same large network of functionally connected areas), we therefore employed functional connectivity in healthy controls. This allowed us to reveal the entire network of regions that are functionally connected to the areas that were reported as contributing significantly to the category fluency performance when directly disconnected. When compared to tractography, functional connectivity has the added advantage of revealing the areas that contribute to the network through both direct, as well as indirect, structural connections.

Principal component analysis indicated that the significant areas contributing to category fluency performance belonged to 3 main functional networks (i.e. factor networks) (**Fig. 4**), which accounted for more than 80% of the total variance of the functional connectivity results.

1
2 The left cingulate clusters (anterior and middle), the right anterior cingulate, the middle
3 frontal gyrus, the thalamus, and the operculum all belonged to the cingulo-opercular network
4 [CO,85] including also the right preSMA, posterior cingulate and the rostral portion of the
5 middle frontal gyrus.
6

7 The middle of the cingulate gyrus and the striatum in the right hemisphere both belonged to a
8 cortico-striatal network [CS,86] involving the right thalamus and striatum.
9

10 Finally, the left MFg, preSMA, IPs, the pars opercularis, the thalamus and the striatum were
11 all involved in a larger, left ventral fronto-parietal network, which also included other areas
12 such as the right preSMA, the frontal eye field and the temporo-parietal junction [VFP,87].
13
14
15
16

17
18 Additional analyses investigated the differences in the functional connectivity of these factor-
19 networks relative to the disconnected status of areas involved in category fluency. Between
20 patients (i.e. connected and disconnected) comparisons revealed significantly lower
21 functional connectivity in the left VFP network ($U = 54.0$, $p = 0.006$) and in the CS network
22 ($U = 63.0$, $p = 0.027$) when anatomically disconnected. The CO network, however, did not
23 show any significant difference ($U = 40.0$, $p = 0.213$). Overall, the strength of the functional
24 connectivity for each patient did not correlate significantly with the fluency performance.
25
26
27
28
29
30

31 32 33 *Structural changes in disconnected regions*

34 Additional exploratory analyses investigated structural changes related to the disconnections.
35 We estimated these changes using two complementary measures: T1w-based cortical
36 thickness to identify fine local volumetric changes and the Shannon entropy of rs-fMRI as a
37 surrogate for the local complexity of the neural networks [75].
38
39
40
41
42
43

44 When compared to controls, patients showed a reduced cortical thickness in the left pars
45 opercularis ($H = 13$; $p = 0.0012$), the MFg ($H = 8$; $p = 0.0143$), the preSMA ($H = 8$; $p =$
46 0.0224), the IPs ($H = 9$; $p = 0.0131$) and the right anterior ($H = 7$; $p = 0.0296$) and middle
47 cingulate gyrus ($H = 23$; $p = 0.000$). When compared to patients with no disconnection,
48 solely the right middle cingulate gyrus survived the Bonferroni-Holm correction for multiple
49 comparisons ($U = 67$; $p = 0.004$). When compared to controls, disconnected patients showed
50 reduced entropy for all regions (all $p < 0.05$, except for the right middle frontal gyrus).
51 However, when compared to patients with no disconnection, none of the comparisons
52
53
54
55
56
57
58
59
60
61
62
63
64
65

1
2 survived the Bonferroni-Holm correction for multiple comparisons. Uncorrected p values are
3 reported as an indication in **table 4, and bar chart in supplementary figure 3.**
4

5 None of these measures correlated significantly with the fluency performance.
6
7

8
9
10 In order to further assess the integrity of the whole network of regions that were functionally
11 connected to the areas reported as having significantly contributed to the category fluency
12 performance, we also extracted the cortical thickness and entropy from the regions that were
13 functionally connected to the disconnected areas. Correlation analyses indicated that a
14 thinner cortex in the ventral fronto-parietal network seeded from the left MFg (Spearman Rho
15 = .464 ± 0.341; p = .004) , IPs (Rho = .475 ± 0.341 ; p = .003) and left
16 oper./striatum/thalamus (Rho = .512 ± 0.341 ; p = .001) corresponded to a reduced
17 performance in category fluency (**Fig. 5**). Additionally, a thinner cortical thickness in the left
18 preSMA functional network (Rho = .376 ± 0.341 ; p = .024) and a higher rs-fMRI entropy
19 (Rho = - .420 ± 0.370 ; p = .019) in the mid cingulate gyrus functional network was
20 associated with poorer performance in category fluency. These two last results, however, did
21 not survive Bonferroni-Holm correction for multiple comparisons.
22
23

24 The same analyses were repeated controlling for age and lesion size and confirmed the results
25 for ventral fronto-parietal network seeded from the left MFg (Spearman Rho = .423; p = .01)
26 , IPs (Rho = .538; p = .001) and left opercularis (Rho = .590 ± 0.341 ; p < .001) corresponded
27 to a reduced performance in category fluency (**Fig. 5**). Additionally, a thinner cortical
28 thickness in the left preSMA functional network (Rho = .439 ; p = .007) and a higher rs-fMRI
29 entropy (Rho = - .420 ± 0.370 ; p = .019) in the mid cingulate gyrus functional network was
30 associated with poorer performance in category fluency
31
32

33 34 35 36 37 38 39 40 41 42 43 44 45 46 47 48 49 **Discussion**

50 A large set of complementary methods can capture the impact of lesions on distant regions
51 and expose the subsequent consequences upon patients' neuropsychological performance.
52 Several of these methods are built directly into our freely available software package
53 *BCBtoolkit*. This package can be employed to measure the pathophysiological mechanisms
54
55
56
57
58

1
2
3
4
5
6
7
8
9
10
11
12
13
14
15
16
17
18
19
20
21
22
23
24
25
26
27
28
29
30
31
32
33
34
35
36
37
38
39
40
41
42
43
44
45
46
47
48
49
50
51
52
53
54
55
56
57
58
59
60
61
62
63
64
65

that cause cognitive deficits, and assess the relationship between these mechanisms and their consequential effects. Here we evaluated the risk of disconnection of classically defined white matter tracts and tested their relationship with category fluency performance. We then employed a tractography-based approach in order to reveal regions that were structurally disconnected by the lesion and assess their relationship with category fluency performance as compared to controls and other patients. Functional connectivity from the disconnected regions revealed large networks of interconnected areas. Within these regions/networks, measures of cortical thickness and of entropy of the rs-fMRI images were correlated to fluency performance, suggesting that some structural changes that occurred within these networks were due to the remote effect of a lesion that led to cognitive impairments. Consequently, the *BCBtoolkit* provided investigators with an ability to quantify the effect of brain damage upon the whole-brain, and explore its relationship to behavioural and cognitive abilities.

The investigation into the contribution of white matter tract disconnection is more than a century old approach and postulates an interruption in the course of white matter tracts in single case patients [88, 89]. Our method provides an anatomical rationale, as well as puts forth a statistical methodology enabling it to be extended to group-level studies. In the case of category fluency performance, this analysis particularly revealed a significant involvement of the anterior and long segments of the arcuate fasciculus, which are implicated in the language network [89-91]. However, these tracts have been defined by their shape for convenience (e.g. uncinata for hook-shaped connections or arcuate for arched-shaped connections) and should not be considered as a single unit, as ultimately, sub-portions could contribute differently to the elaboration of the cognition and behaviour.

Data driven maps of disconnection or ‘disconnectomes’ were consequently produced in order to identify the sub-portion of disconnected tracts and reveal the pattern of cortico-subcortical areas that were disconnected by the lesion. For the first time, we exemplify that this method can go beyond assessing only lesions, and can be employed to assess the relationship between disconnected areas and the patient’s neuropsychological performance. Here, this approach revealed that category fluency performance significantly decreased when several cortical and subcortical clusters were directly disconnected. The observed areas are consistent with

1
2
3
4
5
6
7
8
9
10
11
12
13
14
15
16
17
18
19
20
21
22
23
24
25
26
27
28
29
30
31
32
33
34
35
36
37
38
39
40
41
42
43
44
45
46
47
48
49
50
51
52
53
54
55
56
57
58
59
60
61
62
63
64
65

previous lesion studies on fluency tasks [92]. Furthermore, each area identified as significantly involved in this analysis corresponded, almost systematically, to activation loci derived from *fMRI* studies in healthy controls performing fluency and/or categorisation tasks. This result suggests that the method appropriately identified altered functional networks contributing to the category fluency test. Nonetheless, one might argue that a cascade of polysynaptic events can influence behaviour and that dysfunctional, disconnected areas will also impact other indirectly connected areas.

In order to explore this additional dimension, we calculated the functional connectivity of the previously identified disconnected regions (i.e. clusters). In the case of the present analysis on category fluency performance, we revealed that the disconnected areas belonged to 3 large functional networks (i.e. facto-networks): a left dominant ventral fronto-parietal network, a mirror of the right-lateralized ventral attention network [93], which link key language territories [87] and is associated with executive functions [94, 95]. We additionally showed the involvement of the cingulo-opercular network, a network that interacts with the fronto-parietal control network for the control of goal-directed behaviours [96], which together with cortico-striatal network may also be linked to a reduced performance in fluency tasks [97]. The cingulo-opercular and cortico-striatal networks may also have contributed to performance through the global inertia or the ability of participants to allocate and coordinate resources during the task [98]. Finally, disconnection was associated with a significant reduction of functional connectivity in 2 out of the 3 factor-networks investigated. This is an important result, as functional connectivity appeared to be less significantly impaired in bilateral networks, suggesting that the proportion of the preserved functional network in both of the intact hemispheres may contribute to the strength of functional connectivity.

Changes in connectivity should induce changes in the microstructure of the areas of projection, and provoke cognitive or behavioural consequences. Measures of the cortical thickness revealed a significant thinning for some, but not all, directly disconnected areas. This result may reflect a potential transneuronal degeneration mechanism [42]. However, current limitations in spatial resolution and magnetic resonance imaging signal might have biased this measure in some regions due to changes in myelination in the lower layers of the cortex [99]. Cortical thickness analyses revealed that the left dominant ventral fronto-parietal

1 network, whether it is seeded from MFg, IPs or subcortical structures in the left hemisphere,
2 had a reduced cortical thickness associated to the category fluency performance. This result
3 indicates a strong and encouraging relationship between the integrity of a network derived
4 from measures of cortical thickness and behavioural performances. Future research can
5 benefit from this approach to stratify patients' population and predict potential recovery.
6
7

8
9 Additionally, we explored whether structural changes such as other neural (e.g. synaptic
10 plasticity) or non-neural factors (e.g. altered properties of the vasculature) could also be
11 captured by measures of rs-fMRI entropy. Our results replicated recently published results,
12 showing a strong decrease of entropy in both hemispheres when patients were compared to
13 controls [100]. This indicates a large-scale effect of brain lesion on the overall blood oxygen
14 level dependent dynamic of the brain. Finally, the result between patients (connected and
15 disconnected patients) did not survive the correction for multiple comparisons, suggesting
16 that, although promising, Shannon entropy measures of BOLD may be too noisy of a measure
17 to capture very fine microstructural events with high enough statistical power.
18
19
20
21
22
23
24
25
26

27 Previous reports indicated that *AnaCOM* suffers from lower specificity than VLSM (Rorden
28 et al., 2009). *AnaCOM* compares patients with controls performances, an approach that has
29 previously been criticised [101]. In the context of our study, classical VLSM did not reveal
30 any significant area involved with category fluency. In classical VLSM approaches, non-
31 overlapping lesions are competing for statistical significance, fundamentally assuming that a
32 single region is responsible for the symptoms. In the present study, we follow Associationist
33 principles [102, 103] assuming that several interconnected regions will contribute to the
34 elaboration of the behaviour. By comparing the performance between patients and a control
35 population using *AnaCOM2*, several non-overlapping regions can reach significance, without
36 competing for it. Hence, our results differ theoretically and methodologically from previous
37 approaches. Perhaps more importantly, the network of disconnected areas revealed by
38 *AnaCOM2* is typically considered as functionally engaged for fluency and for categorization
39 in healthy controls.
40
41
42
43
44
45
46
47
48
49
50
51
52

53 Newer multivariate methods have also been shown to provide superior performance
54 compared to traditional VLSM [i.e. support vector regression lesion-symptom mapping, 7,
55 104]. For instance, such approaches have been employed to model the statistical relationship
56
57
58
59
60
61
62
63
64
65

1
2
3
4
5
6
7
8
9
10
11
12
13
14
15
16
17
18
19
20
21
22
23
24
25
26
27
28
29
30
31
32
33
34
35
36
37
38
39
40
41
42
43
44
45
46
47
48
49
50
51
52
53
54
55
56
57
58
59
60
61
62
63
64
65

between damaged voxels in order to reduce false positives. In the *disconnectome maps*, this relationship has been pre-established using an anatomical prior derived from tractography in healthy controls. Therefore, it is not recommended to use multivariate approaches with the *disconnectome maps*, as they might come into conflict with the prebuilt anatomical association between the voxels. Additionally, these approaches require a much larger database of patients than the current study. Future research using large lesion databases will be required to explore the effect of multivariate statistical analysis on *disconnectome maps*.

Multivariate approaches also elegantly demonstrated that false positives can be driven by the vascular architecture [7]. This is an important limitation concerning any voxel and vascular lesion symptom mapping. Here, the group of patients explored included stroke and surgical lesions. Although we cannot exclude the participation of the vascular architecture in the present findings, the heterogeneity of the lesion included in our analyse may have limited this factor. Additionally, the statistical interaction between vascular architecture and the *disconnectome map* results remain to be explored in large database of lesions.

Methods used to estimate cortical thickness has previously been reported to perform poorly in peri-infarct regions, and the quality of the tissue segmentation may be particularly poor for stroke patients [78]. Here, we followed previously published recommendations for applying DiReCT [76] to the data from stroke patients: the lesion was masked out, the tissue segmentations were visually inspected, and manual boundary correction was performed when necessary (see **supplementary figure 2** for an example).

Finally, we applied our methods to the neural basis of category fluency as a proof of concept. The anatomy of category fluency should be, ideally, replicated in a larger sample of patients including adequate lesion coverage of the entire brain to provide a more comprehensive understanding of category fluency deficit after a brain lesion. While gathering such a large dataset of patients with brain lesions would have been impossible to achieve before, it might soon become possible thanks to collaborative initiatives such as the Enigma Consortium stroke recovery initiative (<http://enigma.ini.usc.edu/ongoing/enigma-stroke-recovery/>) [105].

Conclusion

1
2
3
4
5
6
7
8
9
10
11
12
13
14
15
16
17
18
19
20
21
22
23
24
25
26
27
28
29
30
31
32
33
34
35
36
37
38
39
40
41
42
43
44
45
46
47
48
49
50
51
52
53
54
55
56
57
58
59
60
61
62
63
64
65

Overall, using *BCBtoolkit*, researchers and clinicians can measure distant effects of brain lesions and associate these effects with neuropsychological outcomes. However, our methods require the manual delineation of lesion masks, automatization remaining a big challenge, especially on T1-images [105]. Taken together, these neuroimaging measures help discern the natural history of events occurring in the brain after a lesion, as well as assist in the localization of functions. These methods, gathered in the *BCBtoolkit*, are freely available as **supplementary software** at [71].

Data availability

Patients' lesions registered to the reference map MNI152 are available as supplementary material via the BCBlab website [106], and via the Gigascience database GigaDB [107]. However, we are not able to fully share the actual clinical sample data because sharing of the clinical raw data is not covered by the participants' consent. A copy of the consent form as signed by the participants is available via GigaDB.

Availability of supporting source code and requirements

- Project name: BCBtoolkit
- Project home page: <http://toolkit.bcblab.com>
- Operating system(s): Linux, MacOS
- Programming language: Java, Bash, R
- Other requirements: FSL, R, Python 2.7, Numpy
- License: BSD 3-Clause

An archival copy of the supporting source code is also available via GigaDB [107].

•

Authors' contributions

C.F. implemented the methods inside the *BCBtoolkit*, performed the analyses and wrote the manuscript. L.C. created the pipeline for the preprocessing of the resting state and for the functional correlation and revised the manuscript. S.K. conceived and help to upgrade the

1
2
3
4
5
6
7
8
9
10
11
12
13
14
15
16
17
18
19
20
21
22
23
24
25
26
27
28
29
30
31
32
33
34
35
36
37
38
39
40
41
42
43
44
45
46
47
48
49
50
51
52
53
54
55
56
57
58
59
60
61
62
63
64
65

statistical analyses. C.R. collected the neuroimaging data. M.U. and E.V recruited the subjects, collected and built the database of patients and matched healthy controls including the neuropsychological and neuroimaging data and revised the manuscript. E.V. also participated in the conception of the lesion study, and also provided funding for the database acquisition. R.L. provided funding for the study and revised the manuscript. M.T.d.S. wrote the manuscript, provided funding, conceived and coordinated the study, reviewed and collected neuroimaging data.

Acknowledgments

We thank Lauren Sakuma, Roberto Toro, Jean Daunizeau, Emmanuel Mandonnet, Beatrice Garcin, Stephanie J. Forkel and the BCBlab and Brainhack for useful discussions. The authors also thank the participants of this study as well as Prof. Claude Adam, Dr. Carole Azuar, Dr Marie-Laure Bréchemier, Dr. Dorian Chauvet, Dr Frédéric Clarençon Dr. Vincent Degos, Prof. Sophie Dupont, Prof. Damien Galanaud, Dr Béatrice Garcin, Dr. Florence Laigle, Dr Marc-Antoine Labeyrie, Dr. Anne Leger, Prof. Vincent Navarro, Prof. Pascale Pradat-Diehl, and Prof. Michel Wager for their help in recruiting the patients. The research leading to these results received funding from the “Agence Nationale de la Recherche” [grants number ANR-09-RPDOC-004-01 and number ANR-13- JSV4-0001-01] and from the Fondation pour la Recherche Médicale (FRM). Additional financial support comes from the program “Investissements d’avenir” ANR-10-IAIHU-06.

References

1. *Brain Connectivity and Behaviour Toolkit (BCBtoolkit)*, <http://toolkit.bcblab.com/>.
2. Jones, D.K., et al., *Non-invasive assessment of axonal fiber connectivity in the human brain via diffusion tensor MRI*. *Magnetic Resonance in Medicine*, 1999. **42**(1): p. 37-41.
3. Logothetis, N., *What we can do and what we cannot do with fMRI*. *Nature*, 2008. **453**(7197): p. 869-78.
4. Broca, P., *Perte de la parole, ramollissement chronique et destruction partielle du lobe antérieur gauche du cerveau*. *Bull Soc Anthropol*, 1861. **2**: p. 235-238, 301-321.
5. Damasio, H. and A. Damasio, *Lesion analysis in Neuropsychology*, ed. O.U. Press. 1989, New York.
6. Rorden, C., H.O. Karnath, and L. Bonilha, *Improving lesion-symptom mapping*. *J Cogn Neurosci*, 2007. **19**(7): p. 1081-8.

- 1 7. Mah, Y.H., et al., *Human brain lesion-deficit inference remapped*. Brain, 2014. **137**(Pt 9): p. 2522-31.
- 2 8. Bates, E., et al., *Voxel-based lesion-symptom mapping*. Nature Neuroscience, 2003. **6**(5): p. 448-50.
- 3 9. Dronkers, N.F., et al., *Lesion analysis of the brain areas involved in language*
4 *comprehension*. Cognition, 2004. **92**(1-2): p. 145-77.
- 5 10. Karnath, H.O., S. Ferber, and M. Himmelbach, *Spatial awareness is a function of the*
6 *temporal not the posterior parietal lobe*. Nature, 2001. **411**(6840): p. 950-3.
- 7 11. Bird, C.M., et al., *Visual neglect after right posterior cerebral artery infarction*. J
8 *Neurol Neurosurg Psychiatry*, 2006. **77**(9): p. 1008-12.
- 9 12. Husain, M. and C. Kennard, *Visual neglect associated with frontal lobe infarction*. J
10 *Neurol*, 1996. **243**(9): p. 652-7.
- 11 13. Mort, D.J., et al., *The anatomy of visual neglect*. Brain, 2003. **126**(Pt 9): p. 1986-97.
- 12 14. Coulthard, E.J., P. Nachev, and M. Husain, *Control over conflict during movement*
13 *preparation: role of posterior parietal cortex*. Neuron, 2008. **58**(1): p. 144-57.
- 14 15. Volle, E., et al., *The functional architecture of the left posterior and lateral prefrontal*
15 *cortex in humans*. Cereb Cortex, 2008. **18**(10): p. 2460-9.
- 16 16. Volle, E., R. Levy, and P.W. Burgess, *A new era for lesion-behavior mapping of*
17 *prefrontal functions*, in *Principles of Frontal Lobe Function*, S. D.T. and R.T. Knight,
18 *Editors*. 2013. p. 500–523.
- 19 17. Badre, D., et al., *Hierarchical cognitive control deficits following damage to the*
20 *human frontal lobe*. Nat Neurosci, 2009. **12**(4): p. 515-22.
- 21 18. Geschwind, N., *Disconnexion syndromes in animals and man - Part I*. Brain, 1965.
22 **88**: p. 237-294.
- 23 19. Geschwind, N., *Disconnexion syndromes in animals and man - Part II*. Brain, 1965.
24 **88**: p. 585-644.
- 25 20. Carrera, E. and G. Tononi, *Diaschisis: past, present, future*. Brain, 2014. **137**(Pt 9): p.
26 2408-2422.
- 27 21. Finger, S., P.J. Koehler, and C. Jagella, *The Monakow concept of diaschisis: origins*
28 *and perspectives*. Arch Neurol, 2004. **61**(2): p. 283-8.
- 29 22. Corbetta, M., et al., *Neural basis and recovery of spatial attention deficits in spatial*
30 *neglect*. Nature Neuroscience, 2005. **8**(11): p. 1603-1610.
- 31 23. Thiebaut de Schotten, M., et al., *Damage to white matter pathways in subacute and*
32 *chronic spatial neglect: a group study and 2 single-case studies with complete virtual*
33 *"in vivo" tractography dissection*. Cereb Cortex, 2014. **24**(3): p. 691-706.
- 34 24. Thiebaut de Schotten, M., et al., *Visualization of disconnection syndromes in humans*.
35 *Cortex*, 2008. **44**(8): p. 1097-103.
- 36 25. Urbanski, M., et al., *Reasoning by analogy requires the left frontal pole: lesion-deficit*
37 *mapping and clinical implications*. Brain, 2016. **139**(Pt 6): p. 1783-1799.
- 38 26. Cazzoli, D., et al., *The influence of naturalistic, directionally non-specific motion on*
39 *the spatial deployment of visual attention in right-hemispheric stroke*.
40 *Neuropsychologia*, 2016. **92**: p. 181-189.
- 41 27. Piai, V., et al., *Neuroplasticity of language in lefthemisphere stroke: evidence linking*
42 *subsecond electrophysiology and structural connections*. Human Brain Mapping,
43 2017.
- 44 28. Rudrauf, D., S. Mehta, and T.J. Grabowski, *Disconnection's renaissance takes shape:*
45 *Formal incorporation in group-level lesion studies*. Cortex, 2008. **44**(8): p. 1084-96.
- 46
- 47
- 48
- 49
- 50
- 51
- 52
- 53
- 54
- 55
- 56
- 57
- 58
- 59
- 60
- 61
- 62
- 63
- 64
- 65

- 1 29. Fridriksson, J., et al., *Damage to the anterior arcuate fasciculus predicts non-fluent*
2 *speech production in aphasia*. Brain, 2013. **136**(Pt 11): p. 3451-60.
- 3 30. Hope, T.M., et al., *Distinguishing the effect of lesion load from tract disconnection in*
4 *the arcuate and uncinate fasciculi*. Neuroimage, 2016. **125**: p. 1169-73.
- 5 31. Corbetta, M., et al., *Common behavioral clusters and subcortical anatomy in stroke*.
6 Neuron, 2015. **85**(5): p. 927-41.
- 7 32. Griffis, J.C., et al., *Damage to white matter bottlenecks contributes to language*
8 *impairments after left hemispheric stroke*. Neuroimage Clin, 2017. **14**: p. 552-565.
- 9 33. He, B.J., et al., *Breakdown of functional connectivity in frontoparietal networks*
10 *underlies behavioral deficits in spatial neglect*. Neuron, 2007. **53**(6): p. 905-18.
- 11 34. Turken, A.U. and N.F. Dronkers, *The neural architecture of the language*
12 *comprehension network: converging evidence from lesion and connectivity analyses*.
13 Front Syst Neurosci, 2011. **5**: p. 1.
- 14 35. Bonilha, L., et al., *The brain connectome as a personalized biomarker of seizure*
15 *outcomes after temporal lobectomy*. Neurology, 2015. **84**(18): p. 1846-53.
- 16 36. Thiebaut de Schotten, M., et al., *From Phineas Gage and Monsieur Leborgne to*
17 *H.M.: Revisiting Disconnection Syndromes*. Cereb Cortex, 2015. **25**(12): p. 4812-27.
- 18 37. Kuceyeski, A., et al., *Structural connectome disruption at baseline predicts 6-months*
19 *post-stroke outcome*. Hum Brain Mapp, 2016. **37**(7): p. 2587-601.
- 20 38. Yourganov, G., et al., *Multivariate Connectome-Based Symptom Mapping in Post-*
21 *Stroke Patients: Networks Supporting Language and Speech*. J Neurosci, 2016.
22 **36**(25): p. 6668-79.
- 23 39. Kuceyeski, A., et al., *The Network Modification (NeMo) Tool: elucidating the effect*
24 *of white matter integrity changes on cortical and subcortical structural connectivity*.
25 Brain Connect, 2013. **3**(5): p. 451-63.
- 26 40. Boes, A.D., et al., *Network localization of neurological symptoms from focal brain*
27 *lesions*. Brain, 2015. **138**(Pt 10): p. 3061-75.
- 28 41. Munafo, M., *Metascience: Reproducibility blues*. Nature, 2017. **543**(7647): p. 619-
29 620.
- 30 42. Fornito, A., A. Zalesky, and M. Breakspear, *The connectomics of brain disorders*. Nat
31 Rev Neurosci, 2015. **16**(3): p. 159-72.
- 32 43. Feeney, D.M. and J.C. Baron, *Diaschisis*. Stroke, 1986. **17**(5): p. 817-30.
- 33 44. Cowan, W., *Contemporary Research Methods in Neuroanatomy*. 1970: Springer.
- 34 45. Bredesen, D.E., *Neural apoptosis*. Annals of Neurology, 1995. **38**(6): p. 839-51.
- 35 46. Capurso, S.A., et al., *Deafferentation causes apoptosis in cortical sensory neurons in*
36 *the adult rat*. J Neurosci, 1997. **17**(19): p. 7372-84.
- 37 47. Schaechter, J.D., et al., *Structural and functional plasticity in the somatosensory*
38 *cortex of chronic stroke patients*. Brain, 2006. **129**(Pt 10): p. 2722-33.
- 39 48. Xing, S., et al., *Right hemisphere grey matter structure and language outcomes in*
40 *chronic left hemisphere stroke*. Brain, 2016. **139**(Pt 1): p. 227-41.
- 41 49. Gladsjo, J.A., et al., *Norms for letter and category fluency: demographic corrections*
42 *for age, education, and ethnicity*. Assessment, 1999. **6**(2): p. 147-78.
- 43 50. MacPherson, S.E. and S. Della Sala, *Handbook of Frontal Lobe Assessment*. 2015,
44 Oxford: Oxford University Press.
- 45 51. Lezak, M., *Neuropsychological assessment*. 1995, Oxford: Oxford University Press.
- 46 52. Jones, D.K., et al., *Spatial normalization and averaging of diffusion tensor MRI data*
47 *sets*. NeuroImage, 2002. **17**(2): p. 592-617.

- 1 53. Brett, M., et al., *Spatial normalization of brain images with focal lesions using cost*
2 *function masking*. Neuroimage, 2001. **14**(2): p. 486-500.
- 3 54. Nachev, P., et al., *Enantiomorphic normalization of focally lesioned brains*.
4 Neuroimage, 2008. **39**(3): p. 1215-26.
- 5 55. Zhang, Y., M. Brady, and S.M. Smith, *Segmentation of brain MR images through a*
6 *hidden Markov random field model and the expectation-maximization algorithm*.
7 IEEE Trans. Med. Imaging, 2001. **20**: p. 45–57.
- 8 56. Smith, S.M., *Fast robust automated brain extraction*. Hum Brain Mapp, 2002. **17**(3):
9 p. 143-55.
- 10 57. Avants, B.B., et al., *A reproducible evaluation of ANTs similarity metric performance*
11 *in brain image registration*. Neuroimage, 2011. **54**(3): p. 2033-44.
- 12 58. Rojkova, K., et al., *Atlasing the frontal lobe connections and their variability due to*
13 *age and education: a spherical deconvolution tractography study*. Brain Struct Funct,
14 2016. **221**(3): p. 1751-66.
- 15 59. Catani, M., et al., *Short frontal lobe connections of the human brain*. Cortex, 2012.
16 **48**(2): p. 273-91.
- 17 60. Von Der Heide, R.J., et al., *Dissecting the uncinat fasciculus: disorders,*
18 *controversies and a hypothesis*. Brain, 2013. **136**(Pt 6): p. 1692-707.
- 19 61. Duffau, H., et al., *New insights into the anatomo-functional connectivity of the*
20 *semantic system: a study using cortico-subcortical electrostimulations*. Brain, 2005.
21 **128**(Pt 4): p. 797-810.
- 22 62. Catani, M., D.K. Jones, and D.H. ffytche, *Perisylvian language networks of the*
23 *human brain*. Annals of Neurology, 2005. **57**(1): p. 8-16.
- 24 63. Catani, M. and V. Bambini, *A model for Social Communication And Language*
25 *Evolution and Development (SCALED)*. Curr Opin Neurobiol, 2014. **28**: p. 165-71.
- 26 64. Thiebaut de Schotten, M., et al., *A lateralized brain network for visuospatial*
27 *attention*. Nat Neurosci, 2011. **14**(10): p. 1245-6.
- 28 65. *Trackvis*, <http://trackvis.org/>.
- 29 66. Ciccarelli, O., et al., *Diffusion tractography based group mapping of major white-*
30 *matter pathways in the human brain*. NeuroImage, 2003. **19**(4): p. 1545-55.
- 31 67. Thiebaut de Schotten, M., et al., *Atlasing location, asymmetry and inter-subject*
32 *variability of white matter tracts in the human brain with MR diffusion tractography*.
33 Neuroimage, 2011. **54**(1): p. 49-59.
- 34 68. Kinkingnehun, S., et al., *A novel approach to clinical-radiological correlations:*
35 *Anatomo-Clinical Overlapping Maps (AnaCOM): method and validation*.
36 NeuroImage, 2007. **37**(4): p. 1237-49.
- 37 69. *R Core Team 2016*, <https://www.r-project.org/>.
- 38 70. Yarkoni, T., et al., *Large-scale automated synthesis of human functional*
39 *neuroimaging data*. Nat Methods, 2011. **8**(8): p. 665-70.
- 40 71. *Neurosynth*, <http://neurosynth.org/>.
- 41 72. Jenkinson, M., et al., *Improved optimization for the robust and accurate linear*
42 *registration and motion correction of brain images*. Neuroimage, 2002. **17**(2): p. 825-
43 41.
- 44 73. Woolrich, M.W., et al., *Bayesian analysis of neuroimaging data in FSL*. Neuroimage,
45 2009. **45**(1 Suppl): p. S173-86.
- 46 74. Kenney, J., *Mathematics of Statistics*. 1939, London: Chapman & Hall.
- 47 75. Tononi, G., G.M. Edelman, and O. Sporns, *Complexity and coherency: integrating*
48 *information in the brain*. Trends Cogn Sci, 1998. **2**(12): p. 474-84.
- 49
- 50
- 51
- 52
- 53
- 54
- 55
- 56
- 57
- 58
- 59
- 60
- 61
- 62
- 63
- 64
- 65

- 1 76. Das, S.R., et al., *Registration based cortical thickness measurement*. Neuroimage, 2009. **45**(3): p. 867-79.
- 2 77. Tustison, N.J., et al., *Large-scale evaluation of ANTs and FreeSurfer cortical*
- 3 *thickness measurements*. Neuroimage, 2014. **99**: p. 166-79.
- 4 78. Li, Q., et al., *Cortical thickness estimation in longitudinal stroke studies: A*
- 5 *comparison of 3 measurement methods*. Neuroimage Clin, 2015. **8**: p. 526-35.
- 6 79. Shannon, C.E., *The mathematical theory of communication*. 1963. MD Comput, 1997.
- 7 **14**(4): p. 306-17.
- 8 80. Gray, R., *Entropy and Information Theory*. 2011: Springer US.
- 9 81. Ogawa, S., et al., *Brain magnetic resonance imaging with contrast dependent on*
- 10 *blood oxygenation*. Proc Natl Acad Sci U S A, 1990. **87**(24): p. 9868-72.
- 11 82. Biswal, B., et al., *Functional connectivity in the motor cortex of resting human brain*
- 12 *using echo-planar MRI*. Magn Reson Med, 1995. **34**(4): p. 537-41.
- 13 83. Hebb, D.O., *The Organization of Behavior: A Neuropsychological Theory*. 1949, New
- 14 *York: Wiley and Sons*.
- 15 84. de Haan, B. and H.O. Karnath, *'Whose atlas I use, his song I sing?' - The impact of*
- 16 *anatomical atlases on fiber tract contributions to cognitive deficits after stroke*.
- 17 *Neuroimage*, 2017. **163**: p. 301-309.
- 18 85. Sadaghiani, S. and M. D'Esposito, *Functional Characterization of the Cingulo-*
- 19 *Opercular Network in the Maintenance of Tonic Alertness*. Cereb Cortex, 2015. **25**(9):
- 20 *p. 2763-73*.
- 21 86. Voorn, P., et al., *Putting a spin on the dorsal-ventral divide of the striatum*. Trends
- 22 *Neurosci*, 2004. **27**(8): p. 468-74.
- 23 87. Smith, S.M., et al., *Correspondence of the brain's functional architecture during*
- 24 *activation and rest*. Proc Natl Acad Sci U S A, 2009. **106**(31): p. 13040-5.
- 25 88. Lichtheim, L., *On aphasia*. Brain, 1885. **7**: p. 433-484.
- 26 89. Catani, M. and D.H. ffytche, *The rises and falls of disconnection syndromes*. Brain,
- 27 *2005*. **128**(Pt 10): p. 2224-39.
- 28 90. Dronkers, N.F., et al., *Paul Broca's historic cases: high resolution MR imaging of the*
- 29 *brains of Leborgne and Lelong*. Brain, 2007. **130**(Pt 5): p. 1432-41.
- 30 91. Forkel, S.J., et al., *Anatomical predictors of aphasia recovery: a tractography study of*
- 31 *bilateral perisylvian language networks*. Brain, 2014. **137**(Pt 7): p. 2027-39.
- 32 92. MacPherson, S.E., et al., *Handbook of Frontal Lobe Assessment*. 2015, Oxford:
- 33 *Oxford University Press*.
- 34 93. Fox, M.D., et al., *Spontaneous neuronal activity distinguishes human dorsal and*
- 35 *ventral attention systems*. Proc Natl Acad Sci USA, 2006. **103**(26): p. 10046-51.
- 36 94. Parlatini, V., et al., *Functional segregation and integration within fronto-parietal*
- 37 *networks*. Neuroimage, 2017. **146**: p. 367-375.
- 38 95. Power, J.D. and S.E. Petersen, *Control-related systems in the human brain*. Curr Opin
- 39 *Neurobiol*, 2013. **23**(2): p. 223-8.
- 40 96. Gratton, C., et al., *Distinct Stages of Moment-to-Moment Processing in the*
- 41 *Cinguloopercular and Frontoparietal Networks*. Cereb Cortex, 2016.
- 42 97. Chouiter, L., et al., *Partly segregated cortico-subcortical pathways support*
- 43 *phonologic and semantic verbal fluency: A lesion study*. Neuroscience, 2016. **329**: p.
- 44 *275-83*.
- 45 98. Bonnelle, V., et al., *Saliency network integrity predicts default mode network function*
- 46 *after traumatic brain injury*. Proc Natl Acad Sci U S A, 2012. **109**(12): p. 4690-5.
- 47
- 48
- 49
- 50
- 51
- 52
- 53
- 54
- 55
- 56
- 57
- 58
- 59
- 60
- 61
- 62
- 63
- 64
- 65

- 1
2
3
4
5
6
7
8
9
10
11
12
13
14
15
16
17
18
19
20
21
22
23
24
25
99. Wagstyl, K., et al., *Cortical thickness gradients in structural hierarchies*. Neuroimage, 2015. **111**: p. 241-50.
 100. Saenger, V.M., et al., *Linking Entropy at Rest with the Underlying Structural Connectivity in the Healthy and Lesioned Brain*. Cerebral Cortex, 2017. (**in press**)(2017).
 101. Rorden, C., J. Fridriksson, and H.O. Karnath, *An evaluation of traditional and novel tools for lesion behavior mapping*. Neuroimage, 2009. **44**(4): p. 1355-62.
 102. Geschwind, N., *Disconnexion syndromes in animals and man. II*. Brain, 1965. **88**(3): p. 585-644.
 103. Geschwind, N., *Disconnexion syndromes in animals and man. I*. Brain, 1965. **88**(2): p. 237-94.
 104. Zhang, Y., et al., *Multivariate lesion-symptom mapping using support vector regression*. Hum Brain Mapp, 2014. **35**(12): p. 5861-76.
 105. Liew, S.-L., et al., *The Anatomical Tracings of Lesions After Stroke (ATLAS) Dataset - Release 1.1*. bioRxiv, 2017.
 106. *Open Database Brain Connectivity and Behaviour Laboratory (BCBlab)*, <http://opendata.bcblab.com/>.
 107. Foulon, C., et al., *Supporting data for "Advanced lesion symptom mapping analyses and implementation as BCBtoolkit"*. GigaScience Database 2018. <http://dx.doi.org/10.5524/100399>

26 Captions

27
28
29
30
31
32
33
34
35
36
37
38

Fig. 1: Category fluency performance (mean performance with 95% confidence intervals) for patients with (dark grey) or without (light grey) disconnection of each tract of interest. The green intervals indicate the range of controls' performance corresponding to 95% confidence intervals. * $p < 0.05$

39
40
41
42
43
44
45
46
47
48
49
50
51
52
53
54
55
56
57
58
59

Fig. 2: Areas directly disconnected by the lesion that significantly contributed to a decreased score on category fluency task (referred to as "disconnected areas" in the manuscript). a) Representative slices from *disconnectome maps* computed for category fluency performance, blue clusters indicate group average low performance and red high performance. b) Brain areas contributing significantly after correction for multiple comparisons. c) Category fluency performance (mean performance with 95% confidence intervals) for patients with (dark grey) or without (light grey) disconnection of each of the examined cortical regions. The green interval indicates performance in matched controls with 95% confidence intervals. preSMA: presupplementary motor area, IPs: intraparietal sulcus, MFg: middle frontal gyrus, pars Op.: frontal pars opercularis, A: anterior group of thalamic nuclei, VA ventral anterior VLP: ventrolateral posterior, VLa: ventrolateral anterior. * $p < 0.05$ Bonferroni-Holm corrected for

multiple comparisons.

1
2
3
4 **Fig. 3:** Areas classically activated with *fMRI* ($p < 0.01$ FDR corrected) during fluency (pink)
5 and categorization (cyan) tasks. Areas involved in both fluency and categorization are
6 highlighted in dark blue.
7
8
9

10 **Fig. 4:** Functional networks involving the identified disconnected areas, as defined by resting
11 state functional connectivity. Top panel, main cortical networks involving the disconnected
12 areas revealed by a principal component analysis. Bottom left panel, principal component
13 analysis of the raw functional connectivity result. Bottom right panel, strength of the
14 functional connectivity for patients with (dark grey) or without (light grey) involvement of
15 the functional network. CO: Cingulo-opercular network, CS: cortico-striatal network, VFP:
16 Ventral fronto-parietal network. * indicates $p < 0.05$; **, $p < 0.01$
17
18
19
20
21
22
23
24

25 **Fig. 5:** Dimensional relationship between cortical thickness measured in *rs-fMRI*
26 disconnected networks and category fluency. Note that regression lines (in black) and
27 intervals (mean confidence intervals in red) are for illustrative purposes since we performed a
28 rank-order correlation.
29
30
31
32
33
34
35
36
37
38
39
40
41
42
43
44
45
46
47
48
49
50
51
52
53
54
55
56
57
58
59
60
61
62
63
64
65

Table 1: Demographical and clinical data

ID	Age (years)	Education (years)	Gender	Lesion side	Lesion volume (mm ³)	Lesion delay (months)	Aetiology
P01	56	17	F	right	255	7	stroke
P02	55	19	M	left	34374	76	hematoma
P03	46	17	F	left	14847	126	stroke
P04	50	11	F	left	110145	137	surgery
P05	64	14	M	right	59048	119	stroke
P06	32	16	F	right	15946	129	epilepsy
P07	51	11	M	bilateral	113170	54	stroke
P08	70	5	F	left	51530	85	surgery
P09	47	11	M	right	7809	115	hematoma
P10	62	13	F	bilateral	21295	14	hematoma
P11	41	16	M	right	55848	29	surgery
P12	46	12	M	bilateral	2542	51	hematoma
P13	67	15	M	left	4102	133	stroke
P14	49	9	M	bilateral	14929	19	hematoma
P15	36	14	F	right	40854	82	surgery
P16	40	22	F	left	24829	56	hematoma
P17	40	14	M	bilateral	14364	7	hematoma
P18	23	16	F	right	21681	47	surgery
P19	54	22	M	right	51897	48	stroke
P20	71	17	M	left	25779	91	hematoma
P21	23	15	F	right	29513	36	surgery
P22	27	9	F	left	12986	30	surgery
P23	26	13	F	left	2640	19	surgery
P24	32	14	F	left	12653	4	surgery
P25	59	16	F	left	97	9	hematoma
P26	26	13	F	left	26928	32	stroke
P27	58	12	M	left	1026	3	stroke
P29	75	12	F	left	14938	16	hematoma
P30	52	13	F	right	11978	20	surgery
P31	58	12	M	right	13263	21	surgery
P32	62	5	M	right	20281	9	surgery
P33	41	17	M	left	7463	29	surgery

P34	42	17	M	left	24319	6	Infection
P35	60	12	M	right	41897	24	surgery
P36	51	14	F	right	39213	17	surgery
P37	51	12	F	right	8133	48	surgery
P38	33	17	M	right	140947	48	surgery

Table 2: White matter tracts disconnection relationship with category fluency statistical report. Results are not corrected for multiple comparisons. n1, number of disconnected patients; n2, number of spared patients

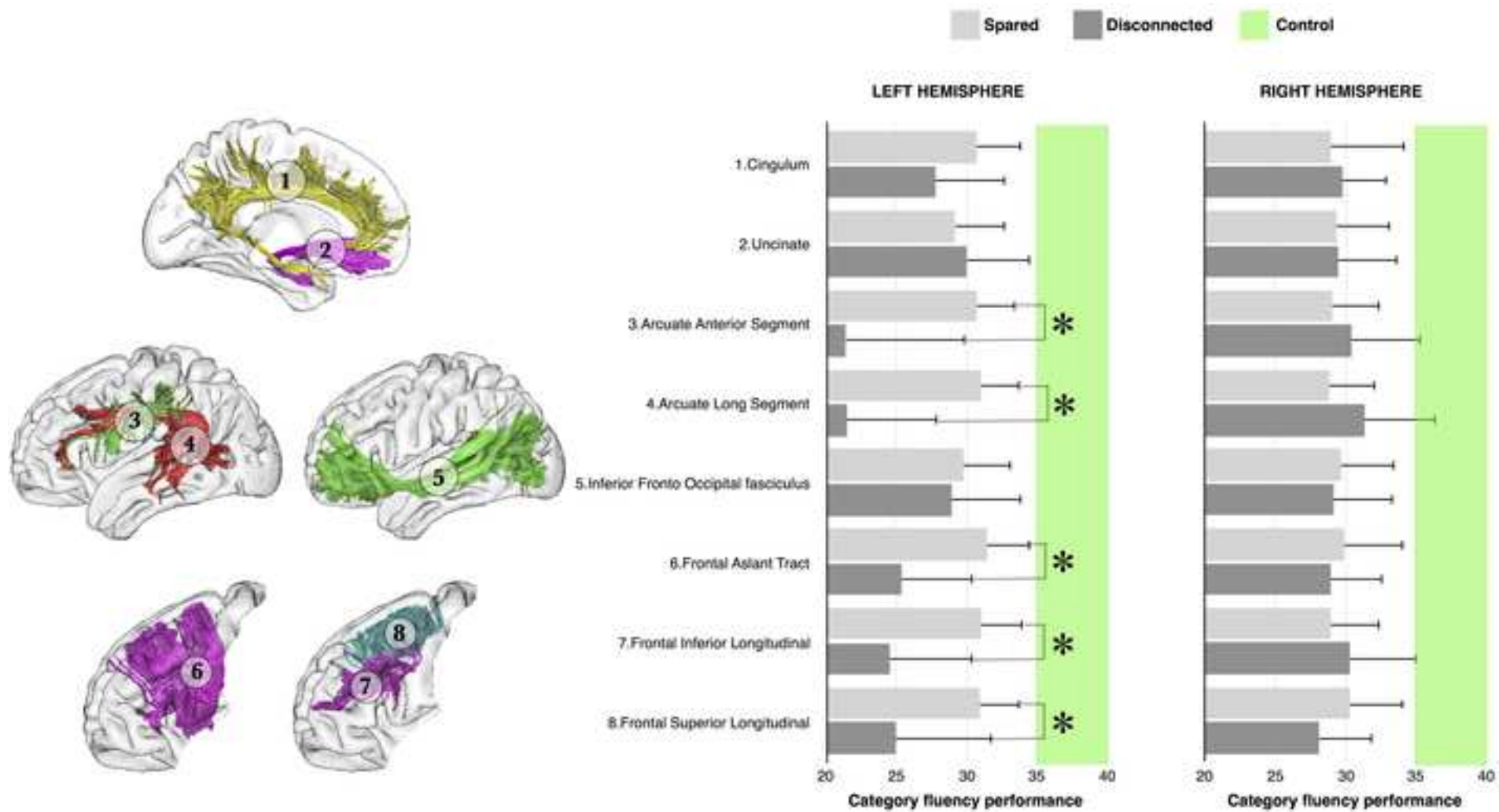
Tracts	3 groups comparison		Patients disconnected and connected		Patients disconnected and controls		Patients connected and controls		n1	n2
	K	P value	U	P value	U	P value	U	P value		
Cingulum Left	19	0.0001	141	0.2035	189	0.0003	277	0.0003	16	21
Cingulum Right	19	0.0001	161	0.5	280	0.0001	187	0.0019	23	14
Uncinate Left	19	0.0001	148	0.3994	176	0.0027	291	0.0001	13	24
Uncinate Right	19	0.0001	167	0.4635	209	0.0004	258	0.0003	17	20
Arcuate Anterior Segment Left	22	0.0000	29	0.0116	12	0.0004	454	0.0001	5	32
Arcuate Anterior Segment Right	19	0.0001	126	0.3855	118	0.0025	348	0.0001	16	21
Arcuate Long Segment Left	23	0.0000	32	0.0059	13	0.0001	453	0.0002	6	31
Arcuate Long Segment Right	19	0.0001	107	0.2559	117	0.0068	349	0.0001	9	28
Inferior Fronto Occipital fasciculus Left	19	0.0001	165	0.5	196	0.0011	271	0.0001	15	22
Inferior Fronto Occipital fasciculus Right	19	0.0001	157	0.3457	199	0.0002	268	0.0004	17	20
Frontal Aslant Tract Left	21	0.0000	90	0.0389	90	0.0001	377	0.0004	11	26
Frontal Aslant tract Right	19	0.0001	155	0.3131	194	0.0001	272	0.0012	18	19
Frontal Inferior Longitudinal Left	21	0.0000	69	0.0216	54	0.0001	413	0.0004	9	28
Frontal Inferior Longitudinal Right	19	0.0001	140	0.3051	171	0.0022	295	0.0001	13	34
Frontal Superior Longitudinal Left	20	0.0000	75	0.0352	73	0.0004	393	0.0002	9	28
Frontal Superior Longitudinal Right	19	0.0001	129	0.1992	120	0.0001	346	0.0005	13	34

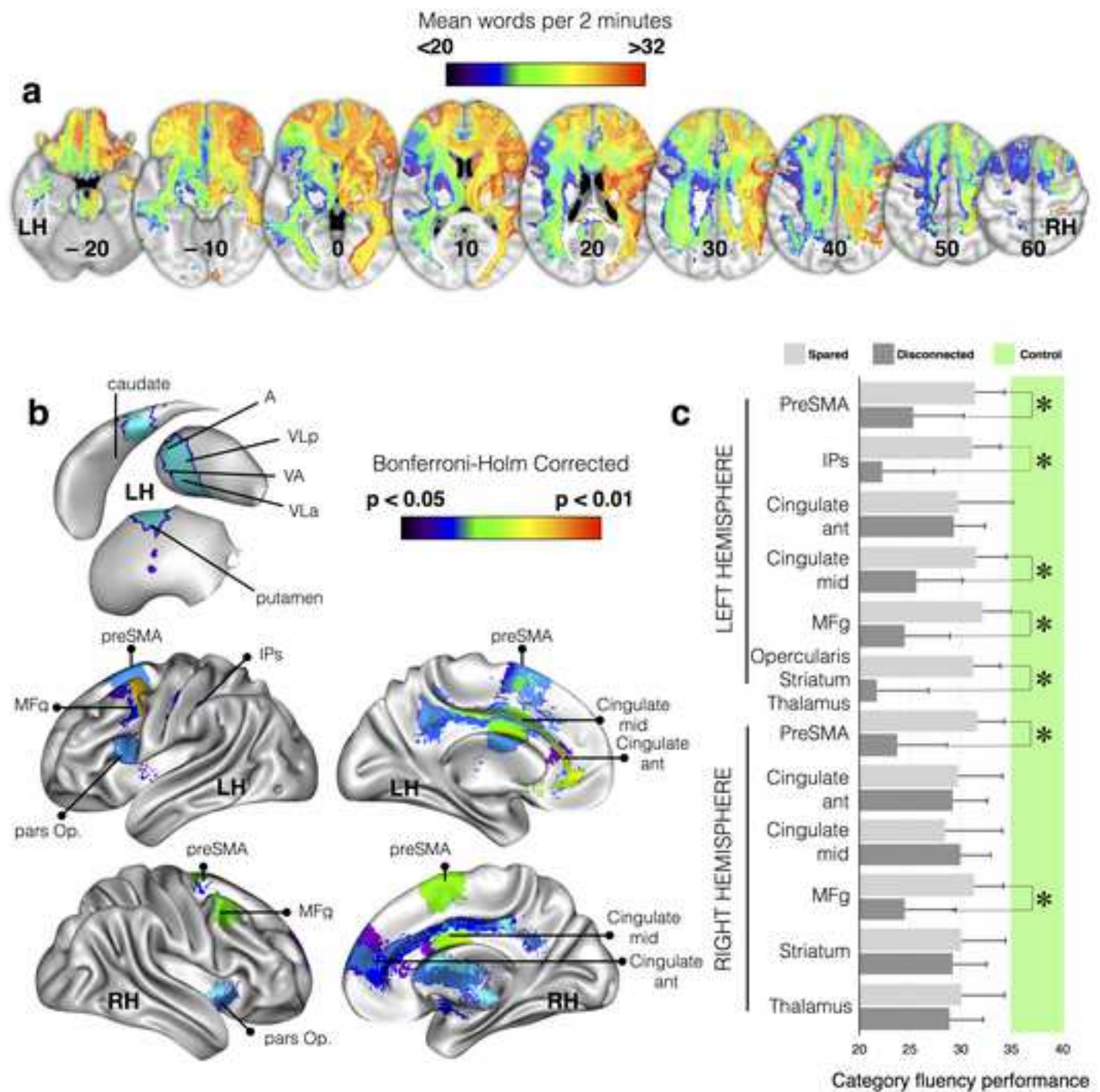
Table 3: Direct disconnection of brain areas relationship with category fluency statistical report. Unless specified, p values are Bonferroni-Holms corrected for multiple comparisons. n1, number of disconnected patients; n2, number of connected patients

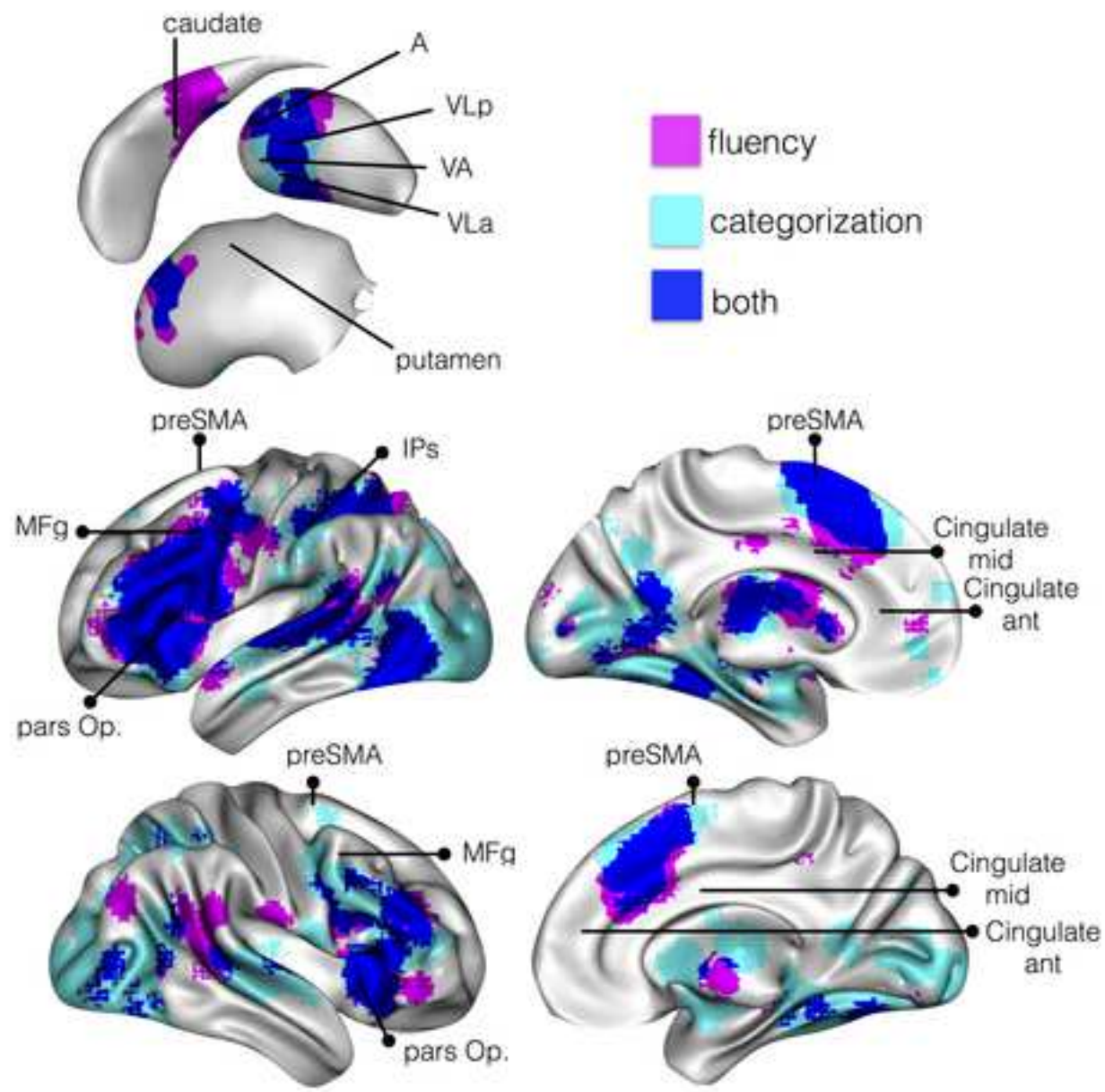
	Disconnected areas	3 groups comparison		Patients disconnected and connected (uncorrected)		Patients disconnected and controls		Patients connected and controls		n1	n2
		Kruskal Wallis	P value	U	P value	U	P value	U	P value		
FLUENCY SCORE LEFT HEMISPHERE	PreSMA	21.34128456	0.0059	212	0.0456	88.5	0.0248	377.5	0.0329	12	25
	IPs	23.35102548	0.0023	172	0.0098	18	0.0295	448	0.0324	7	30
	Cingulate ant	18.6697471	0.0125	160.5	0.7452	304	0.0248	162	0.0329	25	12
	Cingulate mid	21.52289636	0.0054	219	0.0464	95.5	0.0141	370.5	0.0329	13	24
	MFg	23.12826675	0.0026	237	0.0103	81.5	0.0054	384.5	0.0329	13	24
	Opercularis, striatum, thalamus	23.99647373	0.0017	179	0.0043	16	0.0249	450	0.0324	7	30
FLUENCY SCORE RIGHT HEMISPHERE	PreSMA	22.92724537	0.0028	208	0.0130	50.5	0.0138	415.5	0.0329	10	27
	Cingulate ant	18.8698263	0.0125	185.5	0.6470	225	0.0330	241	0.0329	20	17
	Cingulate mid	18.62681983	0.0125	137.5	0.6966	317	0.0415	149	0.0329	25	12
	MFg	22.06856039	0.0042	196	0.0382	54	0.0180	412	0.0329	10	27
	Striatum	18.604408	0.0125	154.5	0.8966	310	0.0313	156	0.0329	14	23
	Thalamus	19.117101	0.0125	192	0.5326	202	0.0248	264	0.0329	14	23

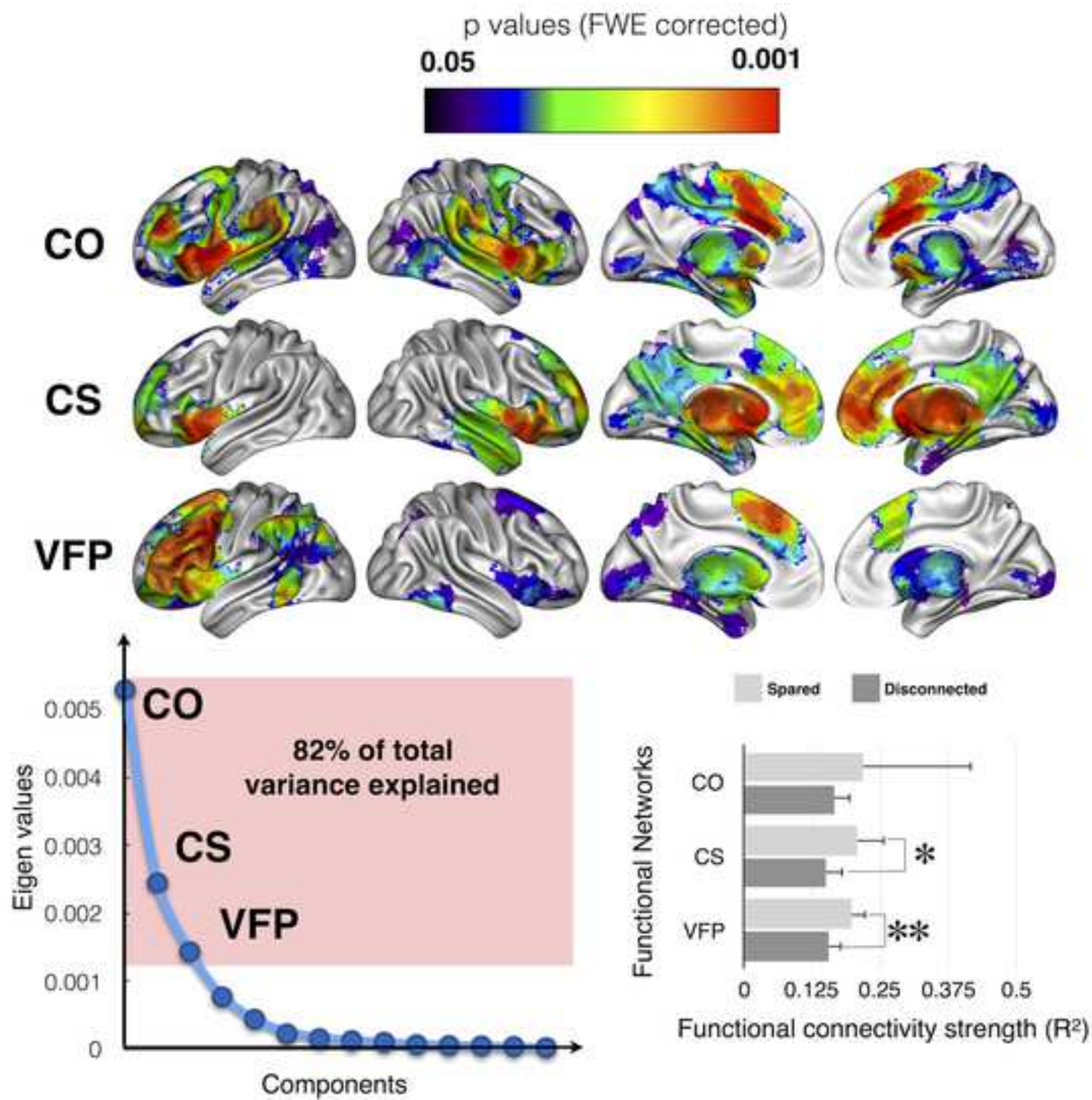
Table 4: Cortical thickness and fMRI entropy measures in disconnected areas. Uncorrected P values. n1, number of disconnected patients; n2, number of spared patients

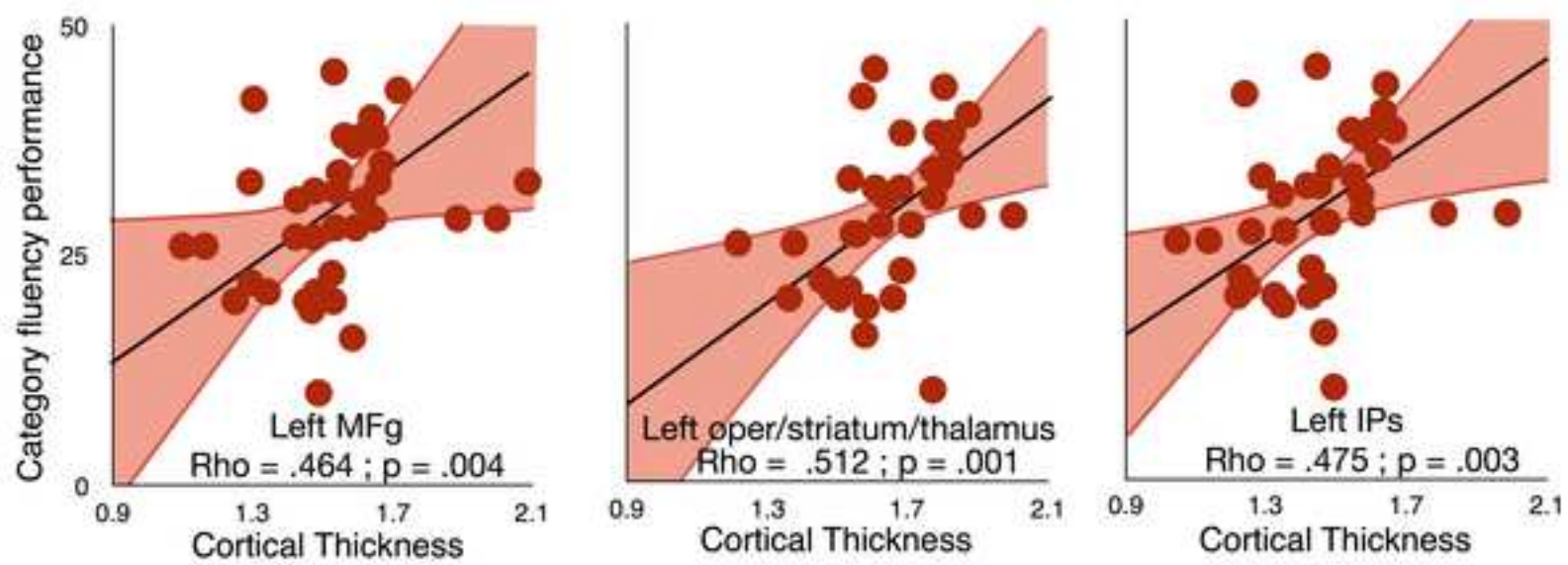
	Disconnected areas	3 groups comparison		Patients disconnected and connected		Patients disconnected and controls		Patients connected and controls		n1	n2
		Kruskal Wallis	P value	U	P value	U	P value	U	P value		
CORTICAL THICKNESS LEFT HEMISPHERE	PreSMA	8	0.0224	109	0.0944	168	0.0057	514	0.0565	12	25
	IPs	9	0.0131	54	0.0251	59	0.0019	667	0.1134	7	30
	Cingulate ant	5	0.0822	110	0.1000	465	0.0175	269	0.2061	25	12
	Cingulate mid	5	0.0759	139	0.2998	278	0.1436	435	0.0137	13	24
	MFg	8	0.0143	109	0.0695	172	0.0028	502	0.0710	13	24
	Opercularis	13	0.0012	40	0.0061	44	0.0006	583	0.0225	7	30
CORTICAL THICKNESS RIGHT HEMISPHERE	PreSMA	4	0.1328	134	0.4931	214	0.1711	523	0.0254	10	27
	Cingulate ant	7	0.0296	167	0.4696	362	0.0191	295	0.0169	20	17
	Cingulate mid	23	0.0000	61	0.0020	223	0.1414	254	0.1415	25	12
	MFg	6	0.0587	116	0.2634	163	0.0359	538	0.0359	10	27
SHANNON ENTROPY LEFT HEMISPHERE	PreSMA	24	0.0000	86	0.2171	85	0.0004	210	0.0000	12	25
	IPs	27	0.0000	40	0.0422	18	0.0002	260	0.0000	7	30
	Cingulate ant	44	0.0000	84	0.1158	109	0.0000	3	0.0000	25	12
	Cingulate mid	36	0.0000	97	0.3029	45	0.0000	127	0.0000	13	24
	MFg	16	0.0004	100	0.4246	125	0.0043	272	0.0003	13	24
	Opercularis, striatum, thalamus	17	0.0002	65	0.3680	75	0.0181	287	0.0001	7	30
SHANNON ENTROPY RIGHT HEMISPHERE	PreSMA	8	0.0177	82	0.2364	117	0.0078	413	0.0243	10	27
	Cingulate ant	55	0.0000	81	0.0640	16	0.0000	4	0.0000	20	17
	Cingulate mid	22	0.0000	111	0.4596	203	0.0001	114	0.0003	25	12
	MFg	22	0.0000	55	0.0497	136	0.0533	209	0.0000	10	27
	Striatum	23	0.0000	110	0.4436	202	0.0001	100	0.0001	14	23
	Thalamus	58	0.0000	67	0.0204	0	0.0000	6	0.0000	14	23













Click here to access/download
Supplementary Material
Supplementary_material.docx

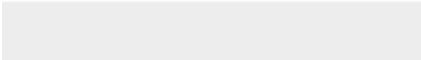
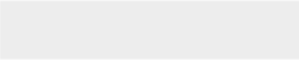








Click here to access/download
Supplementary Material
Supplementary figure 3.docx



Dear dr. Zauner,

Thank you for considering our manuscript untitled ‘**Advanced lesion symptom mapping analyses and implementation as BCBtoolkit**’ for a *technical report* in Gigascience. Additionally, we wish to mention again that we will be happy to be included in the thematic series 'brainhack: Open tools for Brain Science'

Concerning your question, I am afraid there is no protected data access scheme. This is because of the wording of the consent. We are sorry we could not find any way around this.

Please find below our point by point response to the minor suggestions of reviewer 1.

We are looking forward to your assessment.

Sincerely,

Michel Thiebaut de Schotten

1) The He article is cited under lesion-driven tractography but I believe this was a fcMRI study.

Actually, He article includes tractography as well as fcMRI. Results are reported in figure 7B of their paper.

2) The authors could clarify the comment about how much variance in fcMRI data is explained by the three network model.

Thanks for mentioning this was unclear. We modified the text accordingly.

3) It's not clear to me why Shannon entropy is included in the 'Structural changes in disconnected regions' section. It is a functional measure and perhaps a separate paragraph is warranted.

Apologies if this is confusing. Although Shannon entropy was derived from functional MRI, it is not a functional measure since it was acquired at rest (= no function) in order to estimate the intrinsic connectivity. We strongly believe it should remain in the structural section of the manuscript. This point is defended in the method section of the manuscript as follows:

“In the context of rs-fMRI, the entropy measures the local complexity of the Blood Oxygen Level Dependent (BOLD) signal as a surrogate of the complexity of the spontaneous neuronal activity [76, 77]. Since “cells that fire together wire together” [78], for each grey matter voxel Shannon entropy of rs-fMRI can be considered as a surrogate for the complexity of the connections within this voxel and between this voxel and the rest of the brain.”

4) Page 21, line 1. I think the authors meant to comment on adequate lesion coverage of the entire brain and not lesions that involve the entire brain.

Thanks for noticing this mistake! This has now been amended in the manuscript.